Egyptian Geophysical Society
EGS Journal, vol. 2, No. 1, 165-184 (2004)

JUXTAPOSITION AND FAULT SEAL ANALYSIS OF SOME MIXED CLASTIC RESERVOIRS IN EGYPT

Aref Lashin* and Mohamed Abd El-Aal**

* *Geology Department, Faculty of Science, Benha, Zagazig University.*
** *Geology Department, Faculty of Education, Ain Shams University.*

المجاوَرة وتحليل الصدوع الحاجزة لبعض الخزانات الفتاتية المختلطة بمصر

الخلاصة: تلعب الصدوع دورا مهما في تكوين مصائد البترول، حيث تقوم هذه الصدوع بحجز الهيدروكربونات حول مستوياتها عندما تتواجه صخور الخزانات الحاملة للهيدروكربونات ذات الطبيعة البتروفيزيائية والإستراتجرافية المختلفة حول هذه المستويات. و يلقي هذا العمل الضوء على تحليل ودراسة خواص الصدوع القاطعة لبعض التكوينات الفتاتية (الحجرالرملى والطفلة) في مناطق دلتا النيل (غرب أبو قير وأبو ماضي– القرعة) و الصحراء الغربية (أبو سنان) وذلك من خلال إستخدام تسجيلات الآبار والبيانات السيزمية لهذه المناطق. وقد تم حساب وإنشاء تصميم للمجاورة لصخورالخزان حول مستوى الصدع. كما تم إنشاء مجموعة من الأشكال الثلاثية الأبعاد لبعض المعاملات الحاجزة وكذلك نسب الصخور المفتتة بفعل هذا الصدع. كما تم أيضا حساب نسبة الصخورالمفتتة داخل مستوى الصدع. بالإضافة إلى ذ لك تم إختبار بيانات الضغط المسجلة فى الآبار المحفورة على كل من جانبي الصدع وذلك لعمل معايرة لمعاملات الحجز المختلفة التي تم إستنتاجها .ووجد أنه كلما زادت فروق الضغط للخزانات حول مستوى الصدع كلما كان هناك فرصة أكبر لحجزهذه الهيدروكربونات. وبالنسبة لحقلى غرب أبو قيروأبوسنان توجد فروق ضغط كبيرة للخزان حول مستويات الصدوع القاطعة لها مصحوبة بنسب كبيرة من المواد المسحوقة والطفلة المفتتة (١٥–٢٠%) داخل مستويات الصدوع. أما بالنسبة لحقل أبو ماضي– القرعة وجد أن الهيدروكربونات المحجوزة تكون محجوزة نتيجة للأثرالمزدوج الناتج عن الوضع الإستراتجرافي و الصدوع الحابسة فى المنطقة.

ABSTRACT: *Faults play an important role in creating hydrocarbon traps. Sealing along fault planes arises when reservoir/non-reservoir rocks of different petrophysical characters are juxtaposed against each other. This work throw light over the fault seal analysis of some selected mixed clastic reservoirs in the Nile Delta and Western Desert. The potential sealing parameters were checked in three different fields (West Abu Qir, Abu Sennan and Abu Madi-El Qar'a) with different hydrocarbon potentialities (gas and oil) as an attempt to model the sealing attributes in these areas. Different qualitative and quantitative techniques (including seismic and well logging attributes) were used in assessing and evaluating the properties of the fault rock seal types along the faulted reservoirs.*
Number of juxtaposition and 3-D property diagrams (permeability, sealing capacity and relative areas of fault rocks) were constructed along the proposed sealing planes. Moreover, shale gouge ratio (SGR) and smear factor parameters (clay smear potential, CSP and shale smear factor, SSF) were estimated. Pressure data were analyzed on either side of the faults which cut through the potential reservoirs to calibrate the reservoir zones of known petrophysical and sealing parameters. In Abu Sennan and West Abu Qir areas, the structural control of faults is the main sealing factor. In terms of sealing efficiencies, the analyzed reservoirs show two different pressure regimes on either side of the studied faults associated with good sealing parameters (SGR 15-20% and SSF<7). While in Abu Madi-El Qar'a area, sealing is controlled by the combined effect of the deposition of the reservoir (stratigraphic control) and bounding faults (structural control).

INTRODUCTION

The study of the likelihood of a fault to allow fluids to move across the fault plane (leak) or not (seal) is called fault seal analysis. The evaluation of fault sealing forms an important aspect of hydrocarbon exploration, production and reservoir management. Many authors had dealt with faults cutting throw potential reservoirs in terms of evaluating the sealing capacity of these faults like; Allan, 1989, Bouvier et el. (1989), Harding and Tuminas (1989), Knipe (1992a,b and 1993b), Knipe et al. (2004), Chapman and Maneilly (1990), Gauthier and Lake (1993), Yielding (2002), Yielding et al. (1992, 1997, and 1999a,b), Hills and Jones (2003) and Freeman et al. (2004).

Sealing along faults can arise from reservoir/ non-reservoir juxtaposition or by the development of fault rocks, which have high entry pressure. Fault seal in clastic rocks (sand/shale) sequences is broadly predictable, especially when the juxtaposition seal of shale against sand is the main component of trap geometry, (Yielding, 2002). Seals can be considered as membrane seals or hydraulic seals depending on the failure of the membrane seals, which are mainly controlled by the capillary entry pressure (Watts, 1987). A seal which has the capacity to maintain a pressure drop over millions of years is called 'static sealing', while that which maintains a pressure drop over the life time of a single field is called 'dynamic sealing' (Yielding et al., 1999b).

Beside fault seal control, sealing may be also controlled by the stratigraphic condition of the reservoir

of interest, where the manner and shape of deposits (channel fill, lateral variation of facies,...etc) may create good sealing potentialities. A combined effect of sealing (structural/ stratigraphic) can arise in areas where deposition is controlled by the underlying structures (paleo-highs or paleo-lows). Good example of the contribution of paleo-structures to the sealing efficiencies is found in the Nile Delta (Abu Madi-El Qar'a Field).

In the present study, fault seal analysis was applied on three areas (West Abu Qir, Abu Sennan and Abu Madi-El Qar'a) to check the possibility of the applications of these newly introduced techniques and to conclude a final sealing model which could further be applied in another areas with similar petrophysical and structural characteristics. The first step in seal analysis is to identify reservoir juxtaposition areas along the fault plane. The second step is to determine some fault seal related parameters; gouge ratio and smear factor.Watts, (1987) and Knipe, (1992b), recognized a number of mechanisms by which faults can act as a good seal or barrier;

(1) Juxtaposition, where high permeability reservoir units (sand) are juxtaposed against another rock units of different lithology and permeability.

(2) Clay smear potential which is an estimate of the profile thickness of the shales, which have been drawn along the fault zone during faulting. It includes many parameters like clay smear potential (CSP), shale smear factor (SSF) and shale gouge ratio (SGR).

(3) Cataclasis, which is an estimate of the proportions of the crushedfine-grained materials entrained into the fault gouge from wall rocks.

DATASET ANALYSIS

Two different main types of datasets must be prepared first before calculating the sealing capacity. The first is the well logging datasets where complete petrophysical analysis is carried out in wells drilled on either side of the fault plane, while the second is the seismic datasets analysis which deals with the structural attributes of the faults which may act as seal.

Logging Data

Fault seal requires an understanding of the clay content of the sequence which is dissected by a certain fault. So shale volume is of prime interest and must be estimated first prior to the seal analyses. Some other petrophysical parameters like sand and shale beds thicknesses, sand net/gross ratio, porosity, permeability, water and hydrocarbon-bearing zones (oil and/or gas columns) as identified from wells drilled on both sides of the fault, are very important and involved also in the sealing analysis.

Moreover, pressure data are also incorporated in the interpretation to check the pressure difference (Δp) along the fault. Certain cross-fault pressure difference is required to confirm whether the calculated sealing parameters are effective (sealing) or not.

Seismic Data

Seismic data are very important in sealing analysis. The ability of fault to juxtapose reservoir layers of substantially different flow capacity can cause a major baffle to the lateral migration of hydrocarbons (Harris et al., 2002). So, careful choice of the seismic sections passing through the study wells on either side of the examined faults must be done. Determining the upthrown and downthrown fault-horizon intersection for each layer allows an assessment of which reservoir layers are potentially in communication across the fault. Fault parameters (type of fault, dip angle, direction and magnitude of throw) areextracted and used together with other pressure and petrophysical parameters to detect the sealing capacity.

ALGORATHMIS USED IN FAULT SEAL ANALYSIS

A number of different fault-seal algorithms have been published in recent years. Each of which is used to calculate and predict a certain sealing parameter at reservoir-reservoir juxtaposition along the fault plane. The most important parameters, commonly used in seal analysis prediction, are clay smear potential (CSP), shale smear factor (SSF) and shale gouge ratio (SGR). Weber et al. (1978) noticed that faulting of sand–shale sequences can form a continuous multi-layered clay gouge along the median slip plane. In all cases it is very important to perform complete rock typing of the reservoir rocks on either side of the fault plane.

1. Rock Types Prediction

In this study, rock-typing prediction is performed by two methods. The first is the average normal calculations, while the second is the hierarchy algorithm. For a particular depth section, the average sidewall stratigraphy is one which is predicted by the most logs. Using average calculation, rock types can be predicted by combining the different datasets available to create average lithology.

The hierarchical algorithm method ranks the datasets in order of priority, from the most important data to the least important. When the lithology is being calculated, the data with highest priority is used wherever possible. At any depth of the studied section, if the dataset is incomplete, the algorithm will consult the second most important dataset, or if necessary, the datasets of even lower priority. Default host rock types are arranged in terms of priorities from the most important according to the following; high permeable sand, medium permeable sand, low permeable sand, impure sand, shale rich, limestone, cemented sand, anhydrite and coal.

2. Juxtaposition Diagrams

These diagrams are drawn to illustrate the cross-fault reservoir juxtaposition which indicates the different types of rocks juxtaposed against one another. The stratigraphic juxtapositions at any point on the diagram can be established by tracing the footwall stratigraphy (horizontally to the left) and the hangingwall stratigraphy (down along inclined lines) and then back to the stratigraphic column that borders the diagram. Fig. (1) shows an example (Kinpe, 1997) which identifies the stratigraphic unit A that has moved down the fault plane past other lithologies to be juxtaposed against another lithologies/stratigraphic unit D now being horizontally to the left.

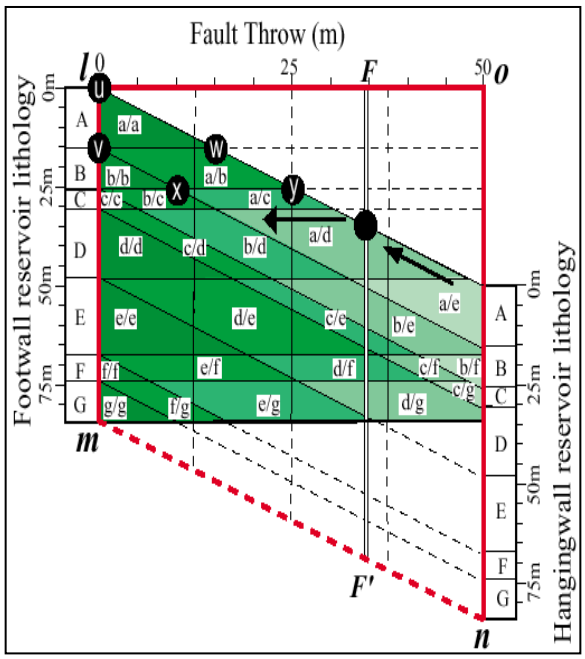

Fig. (1): Illustrates the idea of juxtaposition diagram.

3. Clay Smear Potential (CSP)

While studying the Nunn River field in the Niger Delta, Bouvier et al. (1989) described a clay smear potential (CSP) as a means of estimating the relative amount of clay that has been smeared from individual shale source beds at a certain point along a fault plane.

They calibrated their calculation against actual sealing and non-sealing faults and found that CSP increases with increasing the thickness and number of the displaced source shale beds past a particular point along the fault plane, while it decreases with increasing fault throw. Recently, clay smear potential has been more definitely expressed by Fulljames et al. (1996) as follows:

$$\text{CSP} = \sum \frac{(\text{shale bed thickness})^2}{\text{Distance from source bed}} \quad \text{.....(1)}$$

In simple cases (Fig. 2), where only one source shale bed is present, the smear distance from the source bed is measured from a point nearly lying in the mid of the offset between the source bed in the upthrown side and the corresponding downthrown side.

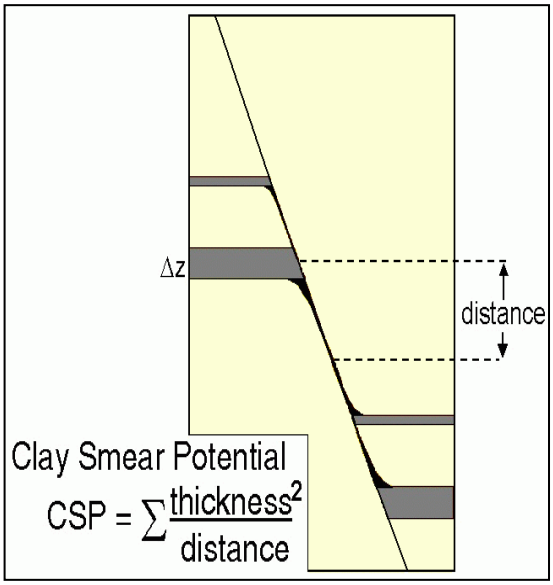

Fig. (2): Clay smear potential.

As the point is not typically in the middle, so it will be somewhat nearer to either the upthrown or the downthrown terminations and the distance is measured from the nearest termination. The measured clay smear potential values are divided by Bouvier et al. (1989) and Jev et al. (1993) into low, medium and high.

In case of multisource shale beds of different thicknesses, the smear distance will differ according to the thickness and the position of each bed from the measuring point and the net clay smear potential will be the summation of the individual smear potential relative to each bed. Low smear potential means little chance for the presence of good, continuous clay smear seals which could enable hydrocarbon entrapment. CSP values less than 15 are considered non-sealing while those more than 30 are regarded as good sealing.

Yielding et al. (1997) suggested that the expression of the (CSP) can be considered in a generalized smear factor (SF) equation as follows:

$$\text{SF} = \sum \frac{(\text{shale bed thickness})^n}{\text{Distance from source bed}^m} \quad \text{.....(2)}$$

The exponents *m* and *n* can be treated as variables whose values can be calibrated and derived from experimental and field studies.

4. Shale Smear Factor (SSF)

Based on their observations of abrasion smears in a lithified sequence, Lindsay et al. (1993) proposed a shale smear factor (SSF) which constrains the continuity of the smear along the fault plan (Fig. 3). They used the following equation:

$$SSF = \frac{\text{Fault throw}}{\text{Shale layer thickness}} \quad \ldots\ldots\ldots (3)$$

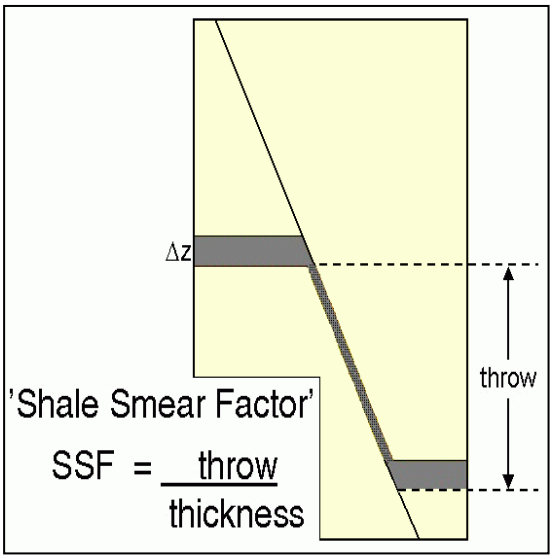

Fig. (3): Shale smear factor.

5. Shale Gouge Ratio (SGR)

Shale gouge ratio (SGR) is another important parameter, which as rapidly becomes a standard methodology for fault seal assessment. CSP and SSF are simple algorithms deepened mainly on the thickness and the offset of individual shale beds in the homogeneous reservoir. So in case of thick heterogeneous sequences it will be difficult to apply such algorithms directly.

Shale gouge ratio (SGR) has the advantage of being applicable in either bed-by-bed reservoirs or as a zonal average value of shale volume when the clays are dispersed through the sandstone units. At each point on the fault plane, SGR is an estimate of the net shale content that has slipped past that point on the fault plane. It can be measured using the following equation (Yielding et al., 1997):

$$SGR = \frac{\sum(\text{Shale bed thickness})}{\text{Fault throw}} .100\% \ldots..(4)$$

So shale gouge ratio (SGR) represents the proportions of shale or clay that might be entrained in the fault zone by a variety of mechanisms. The more shaly wall rocks will increase the amount of shale in the fault zone, hence high capillary pressure.

In case of thick reservoir zone (Fig. 4) where the faulting affecting a zone of beds rather individual simple beds another treatment for the shale gouge ratio (SGR) can be used:

$$SGR = \frac{\sum(\text{zone thickness}).(\text{zone clay fraction})}{\text{Fault throw}} .100\% \quad \ldots\ldots.(5)$$

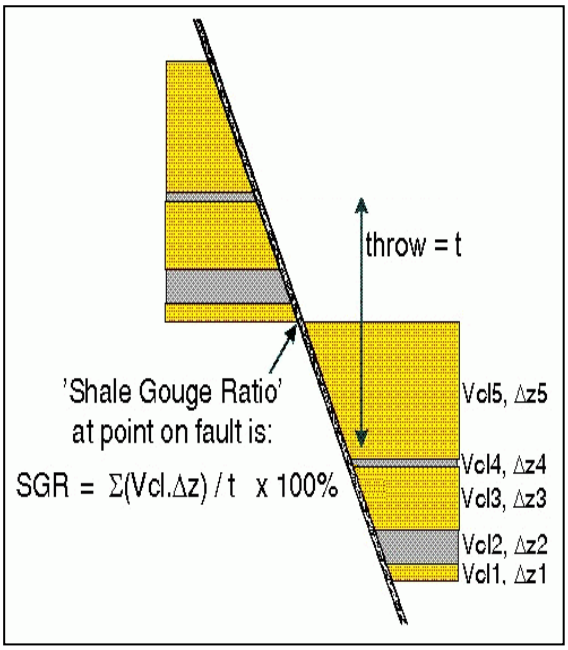

Fig. (4): Shale gouge ratio.

3-D PROPERTY DIAGRAMS

A number of 3-D property diagrams were constructed along the proposed sealing fault plane. Each of which is used to highlight certain fault related property. The most important of these are the permeability, sealing capacity and the relative areas of fault rocks.

1. Permeability Diagram

Determining of permeability along the fault plane is of prime interest. Permeable zones, when found, represent the most capable hydrocarbon-bearing zones of formation which could be sealed and prevented from escaping by a sealing closed fault.

3-D permeability diagram is a representation of the regions in the sealing diagram which correspond to high permeability. The height of each 3-D column is proportional to the logarithmic value of the permeability (mD).

2. Sealing Capacity Diagram

Sealing capacity diagram is very important as it clarifies in 3-D representation the corresponding regions of the faults rocks, which have good sealing capacities. To construct the sealing diagram, it is very important to specify the interfacial angle tension (dyne/cm) and the contact angle (degrees) for two assumed fluid systems (hydrocarbon/water and mercury/air) in the studied section. The interfaces between these two fluid systems together with the densities of water and hydrocarbon (g/cc) must be determined first. The sealing capacity H can be defined as follows:

$$H = \frac{\gamma_h \cos\theta_h}{0.433\ (\rho_w - \rho_h)\gamma_m \cos\theta_m} .Pd_m \ldots..(6)$$

Where:

H is the sealing capacity height.

ρ_h and ρ_w denote the density (g/cc) of the hydrocarbon and water, respectively.

3. Relative Areas of Fault Rocks Diagram

The relative areas of fault rocks diagram is derived from the sealing diagram by a vertical redistribution of the fault rock types present at any fault throw. The fault rock types are then vertically ordered starting with sand rich fault rocks at the base of the diagram and continued vertically to sand poor fault rocks with any additional unit fault rocks stacked at the top.

Any regions of the sealing diagram where the fault rock types are not known appear as white sections at the top of the diagram.

APPLICATIONS

In the present work fault seal analysis was applied on three different areas (Fig. 5) as an attempt to construct a sealing model for each area.

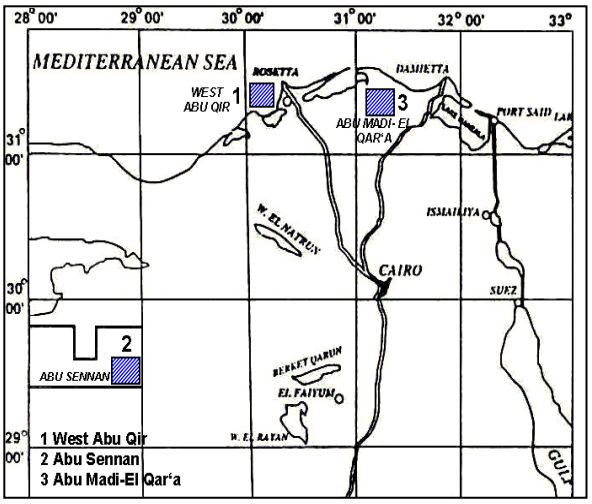

Fig. (5): Location map of the study areas.

The target reservoirs (Abu Madi Formation) in two different fields in the Nile Delta (Abu Madi-El Qar'a and West Abu Qir) are mainly gas- bearing, while in the third field (Abu Sennan in the Western Desert), the target is chosen to be oil-bearing (Abu Roash G Member). Lithologically these reservoirs consist mainly of mixed clastic deposits (sand and shale) and with some carbonate intercalations as in case of Abu Roash G Member. The studied wells are selected on either side of the fault planes which dissect these reservoirs.

Being constructed, the sealing model could further be extended and applied with more details for each area separately to detect the areas of good sealing efficiencies and the directions along which hydrocarbons (oil and/or gas) could migrate and finally the best area for hydrocarbon accumulations.

CASE 1: WEST ABU QIR GAS FIELD

This field was discovered in Oct. 1989 by drilling and testing W. Abu Qir 1X well. Structurally, the field is an elongated E-W structure consisting of two culminations (western and eastern). The first western culmination encloses W. Abu Qir-1X and W. Abu Qir-3X wells, while the second is located southeast of the structure and encloses W. Abu Qir-4X (EGPC, 1994). Fault seal analysis was carried out in this field by chosing two wells namely, W. Abu Qir-1X and W. Abu Qir-4X wells. Each of these two wells exists in a different structure culmination and separated by normal fault.

Fig (6) shows an interpreted seismic section cutting through the study wells. W. Abu Qir-4X well is located in the downthrown side of a normal fault separating the two wells. The fault dips in a southeast direction and attains maximum throw of 80 ft (24 m).

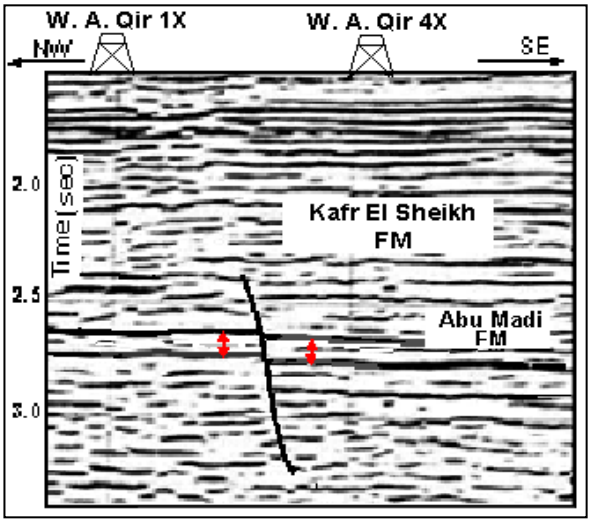

Fig. (6): Seismic section cutting through the study wells in West Abu Qir area.

1. Petrophysical Analysis

The petrophysical analysis of Abu Madi Formation in West Abu Qir field reveals that gases, when found, are usually encountered in two different zones. Fig. (7) illustrates the gas effect regarding W. Abu Qir-1X as an example and the various logging datasets used in the evaluation.

Moreover, the petrophysical analysis of W. Abu Qir-1X well is displayed on Fig. (8). It shows that, two gas-bearing zones are recognized in the upper and lower middle parts of Abu Madi Formation, in two different levels characterized by their clean sand content and separated from the overlying and underlying lithologies by some evaporite interbeds.

The reservoir quality in these two zones is very good in terms of good permeability and effective porosity, and high hydrocarbon content.

The different deduced petrophysical parameters for the two gas-bearing zones in the two studied wells are listed in Table (1).

Table (1): Average main reservoir characteristics of the gas bearing-zones in W. A. Qir-1X and W. A. Qir-4X wells.

Well	Zone	Depth (ft)	Petrophysical Analysis			
			V_{sh}	ϕ_e	S_W	S_H
W. A. Qir - 1X	Z1	9198-9276	0.02	0.24	0.24	0.76
	Z2	9358-9388	0.03	0.22	0.42	0.58
W. A. Qir - 4X	Z1	9255-9310	0.19	0.16	0.74	0.26
	Z2	9465-9545	0.08	0.18	0.79	0.21

2. Sealing Analysis

Fig. (9) shows the constructed juxtaposition diagram along the fault plane regarding West Abu Qir area. The footwall reservoir (FW) lithology in the juxtaposition diagram is correlated with the actual lithology of W. A. Qir-1X in the upthrown side of the fault plane. The hierarchical rock typing classified Abu Madi Formation into seven rock units from A to G of which units B and D are the main gas-bearing zones. As indicated from the host rock lithology key, these two units are characterized by high sand/shale ratio, low shale volume and good porosity and permeability values.

A more detailed picture for the possible juxtaposed rock units and their sealing capacities is exhibited in the sealing diagram (Fig. 10). The diagram shows that part of the permeable sand (high, medium and low) of the gas-bearing zone-1 (unit B) in the footwall is still facing permeable sand in the hangingwall (permeable sand in the FW against permeable sand in the HW not past other lithology). On the other hand, part of the permeable sand in the same zone is juxtaposed against another lithology (permeable sand in the FW against permeable sand in the FW past other lithology).

High smear potential (shale and anhydrite) is indicated between depths 9275 ft and 9350 ft, where the fault attains its maximum throw. Good sealing capacities were found above the two gas zones as indicated by the high potential phylosilicates rich fault rock (high clay smear potential) which capping and diagonally facing the two permeable gas zones along the fault plane. In front of the gas-bearing zone-2 in the footwall lithology (unit D) and at depth 9370 ft, a medium to low permeable sand unit is juxtaposed against another lithology in the hangingwall (unit B). This unit undergoes the maximum sealing capacity in the constructed sealing diagram, which could affect the reservoir lithology in the study area.

The 3-D logarithmic permeability and sealing capacity diagrams are shown in Fig. (11 A & B). In the 3-D permeability diagram, the logarithmic permeability scale gives high permeability values up to 3.0 mD for the two gas-bearing sand zones from one hand and for the juxtaposed unit from the other hand, meanwhile very low values are recorded for the fault rock lithology. The 3-D sealing capacity diagram shows that the high sealing fault rock lithology which has big column height and high smear factor, is interbedding the reservoir sand lithology and enhances good sealing and coating diagonally along the fault plan.

Shale gouge ratio (SGR) diagram (Fig. 12) illustrates that low SGR values are recorded in front of the sand zones (B, D and F) and the juxtaposed sand unit. Meanwhile, very high SGR values are measured (SGR >20%) for the other lithology especially above and below the gas-bearing zone-1 (SGR > 40%).

The minimum smear factor diagram (Fig. 13) classifies the rock lithology along the fault planes, in terms of SSF values, into reservoir rocks with good sealing capacities (SSF < 7), reservoir rocks with little or no sealing capacities (SSF > 7) and non reservoir rocks (fault wall lithology). The recorded SSF values for fault wall lithology in front of the two gas-bearing zones and around the juxtaposed reservoir unit range between 4%-7%. Moreover, the relative fault area diagram (Fig. 14) illustrates that, the fault wall consists mainly of shale rich fault rock, high potential shale and impure framework fault rocks. Some anhydrites are also found.

CASE 2: (ABU SENNAN -GPT FIELD)

GPT field is located in Abu Sennan area, about 10 km east of Abu Gharadig field. The structure of this area was interpreted by using the seismic lines of GPC survey which was carried out in 1980. Two wells (GPT-1 and GPT-14) were used in the sealing analysis.

The Abu Roash Formation in this area includes four target reservoirs (A/R B, D, E and G) which are mainly carbonate in composition. The Abu Roash G Member is used in the analysis, as it is nearly the only reservoir in this area which is mainly composed of clastics with minor interbeds of carbonates. The sealing capacity of a normal fault cutting through A/R G Member between GPT-1 well (upthrown side) and GPT-14 well (downthrown side) is investigated. The interpreted seismic section (Fig. 15) shows that the fault dip direction is to the southeast and the magnitude of throw is about 71 m (233 ft).

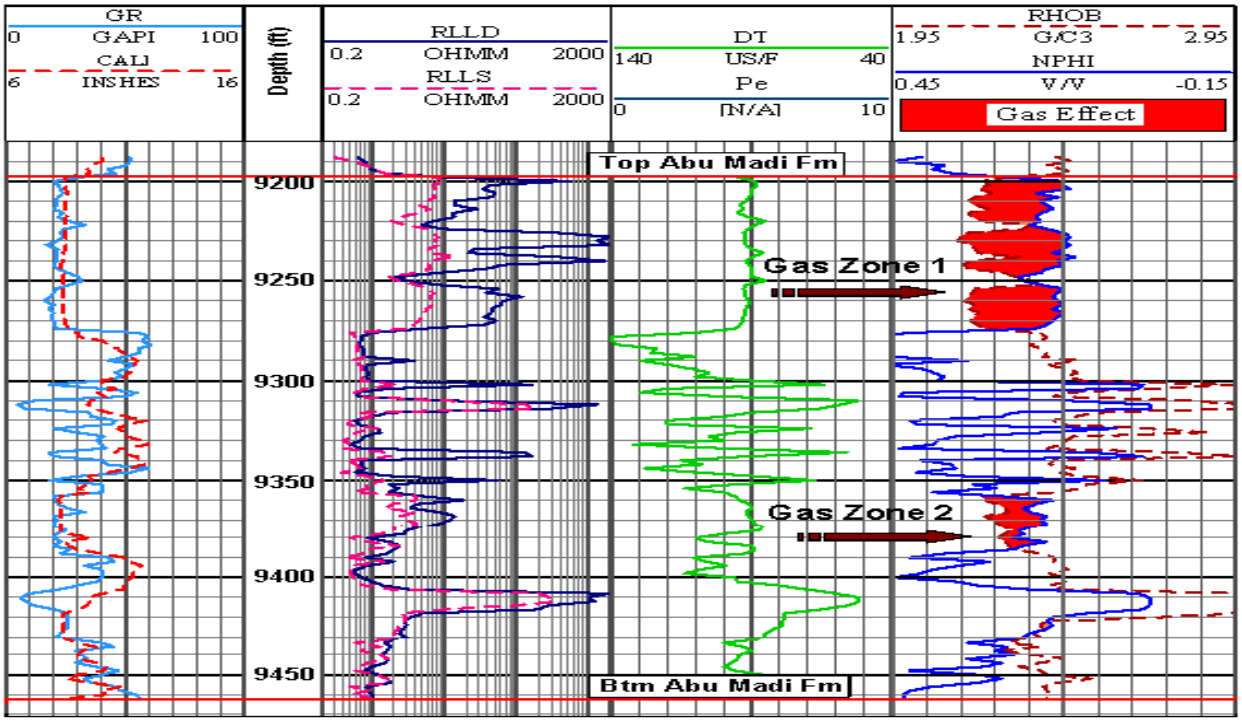

Fig. (7): Gas effect is shown at two zones in W. Abu Qir-1X well.

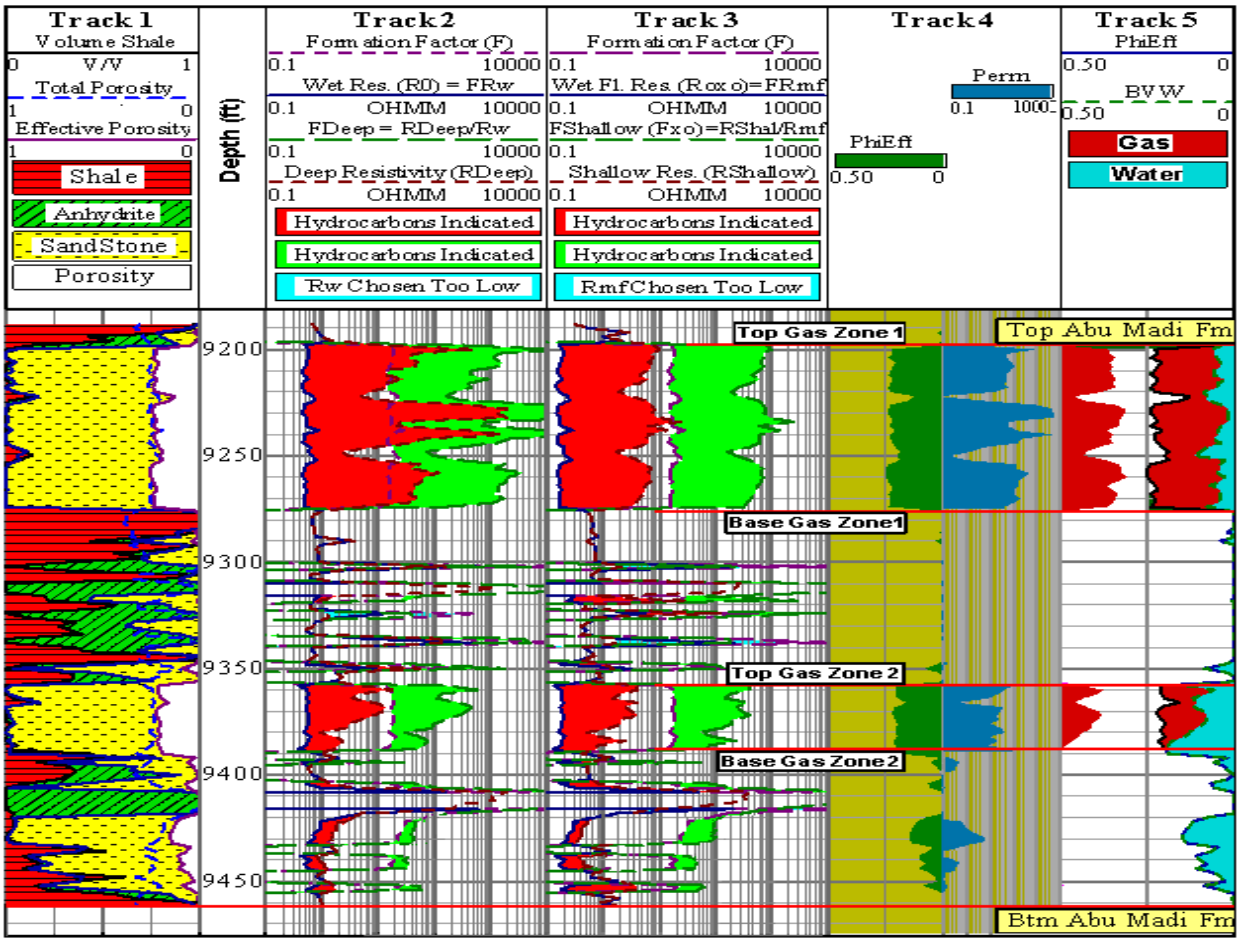

Fig. (8): Petrophysical analysis of W. Abu Qir-1X well.

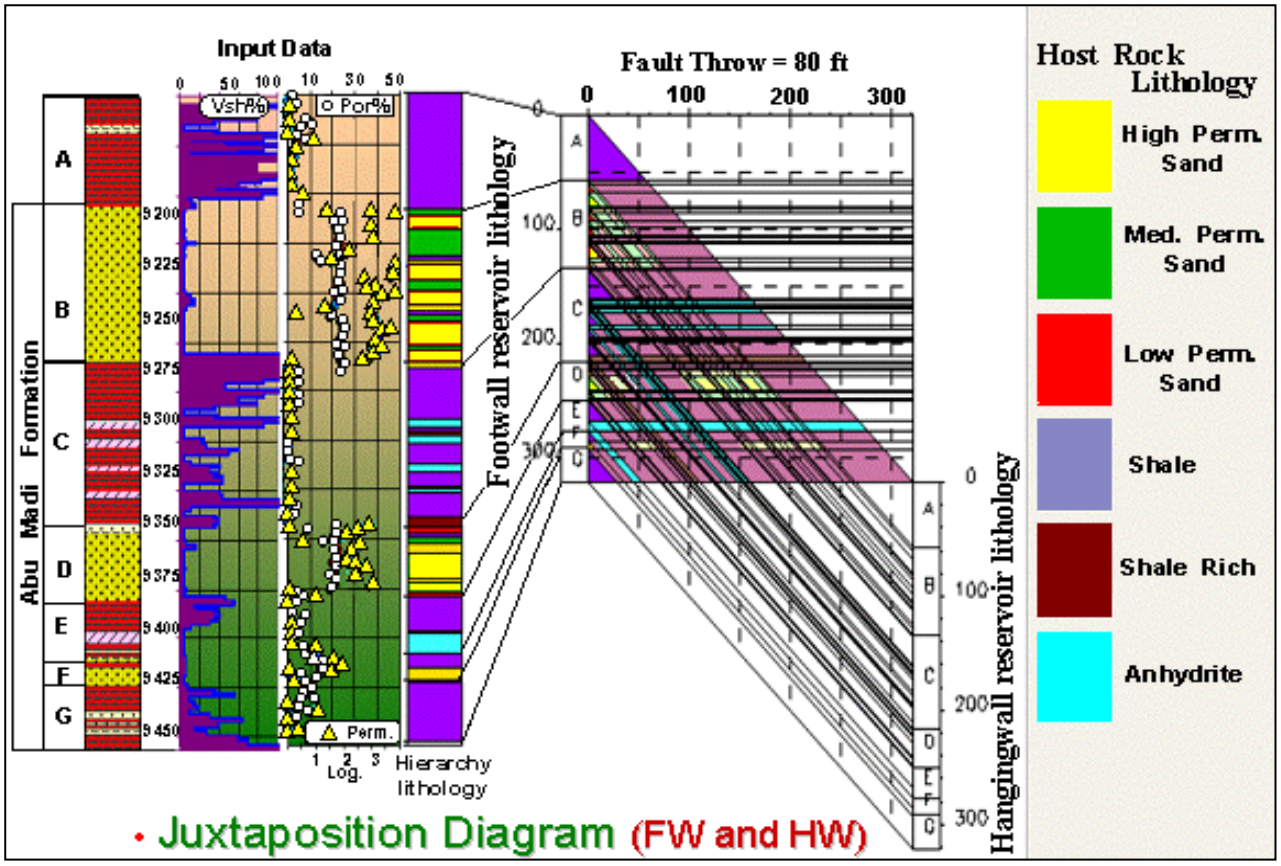

Fig. (9): Juxtaposition diagram of W. Abu Qir area.

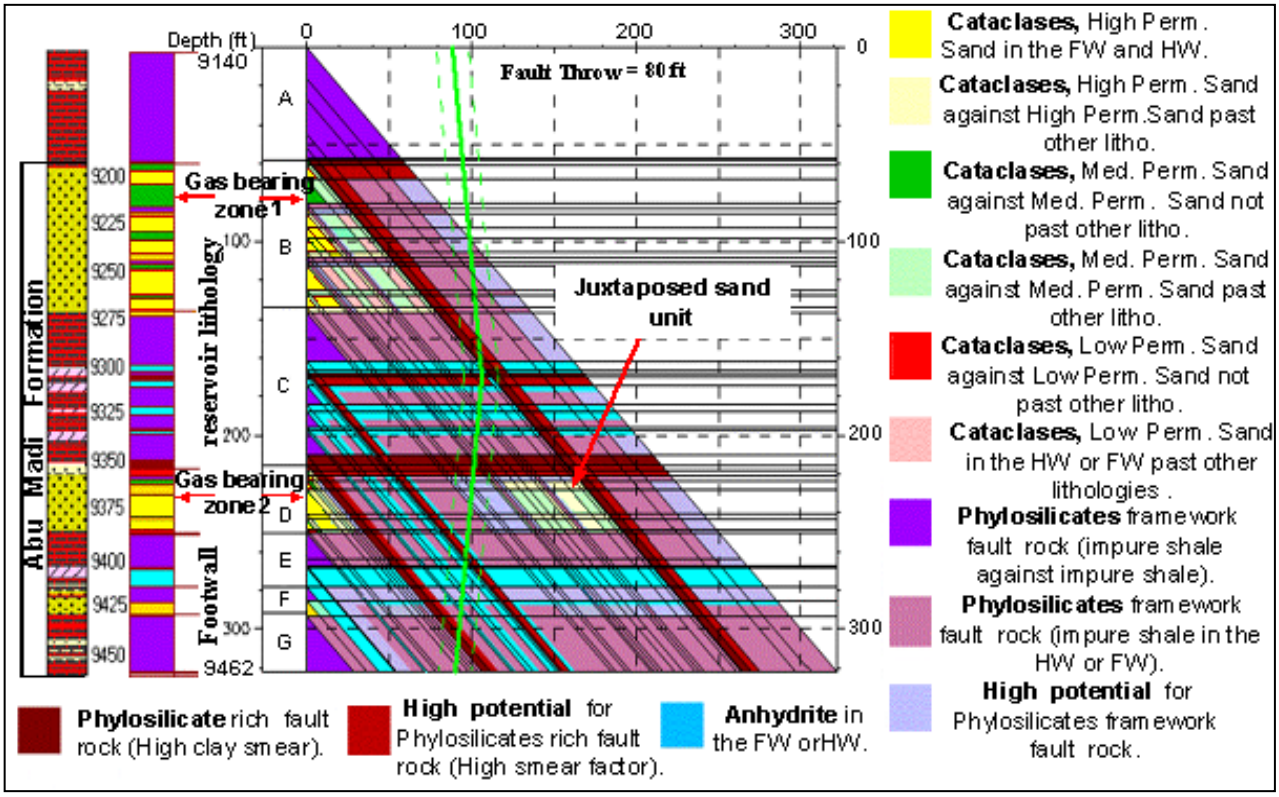

Fig. (10): Sealing capacity diagram of W. Abu Qir area (FW).

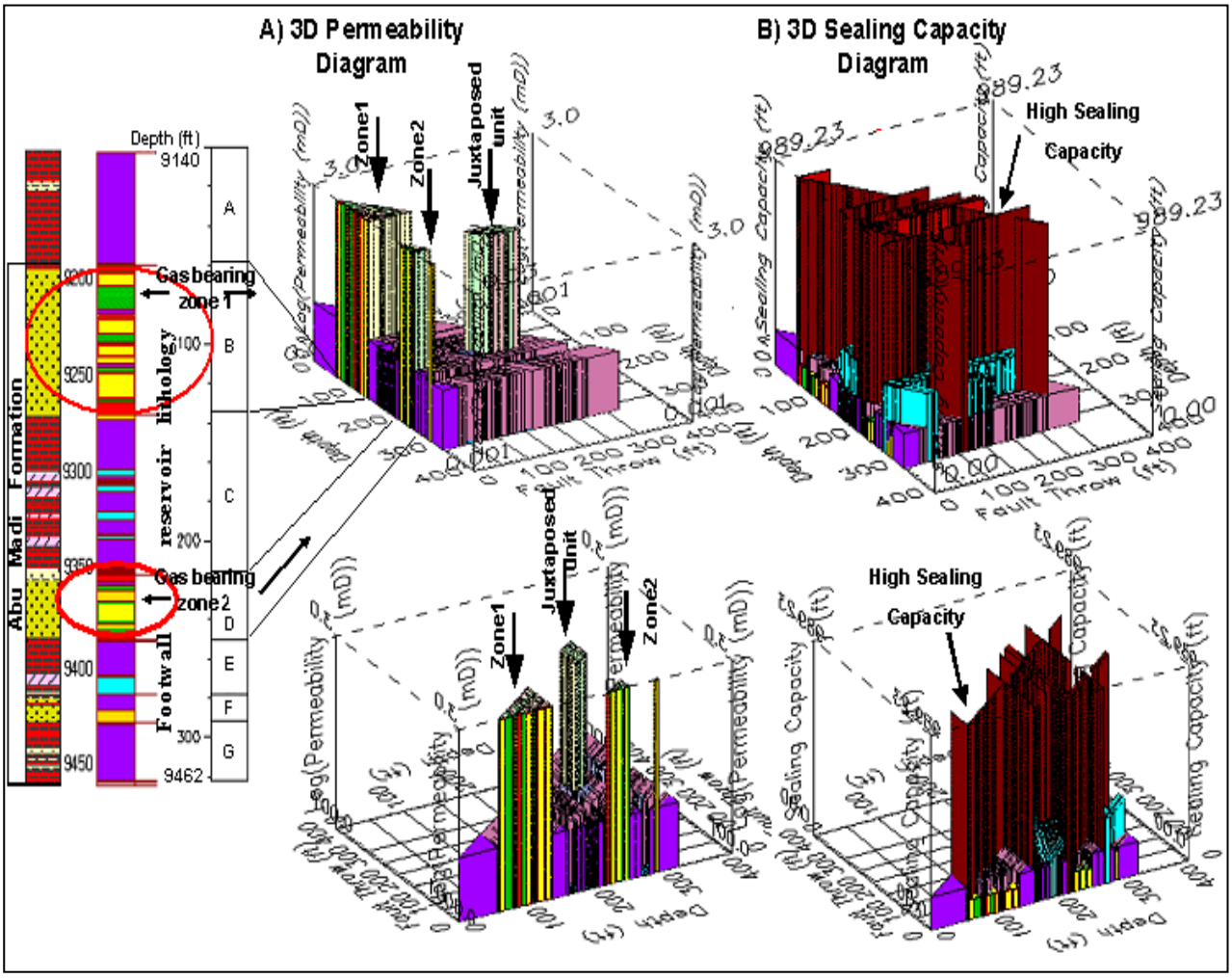

Fig. (11): 3-D permeability and sealing capacity diagrams of W. Abu Qir area (FW).

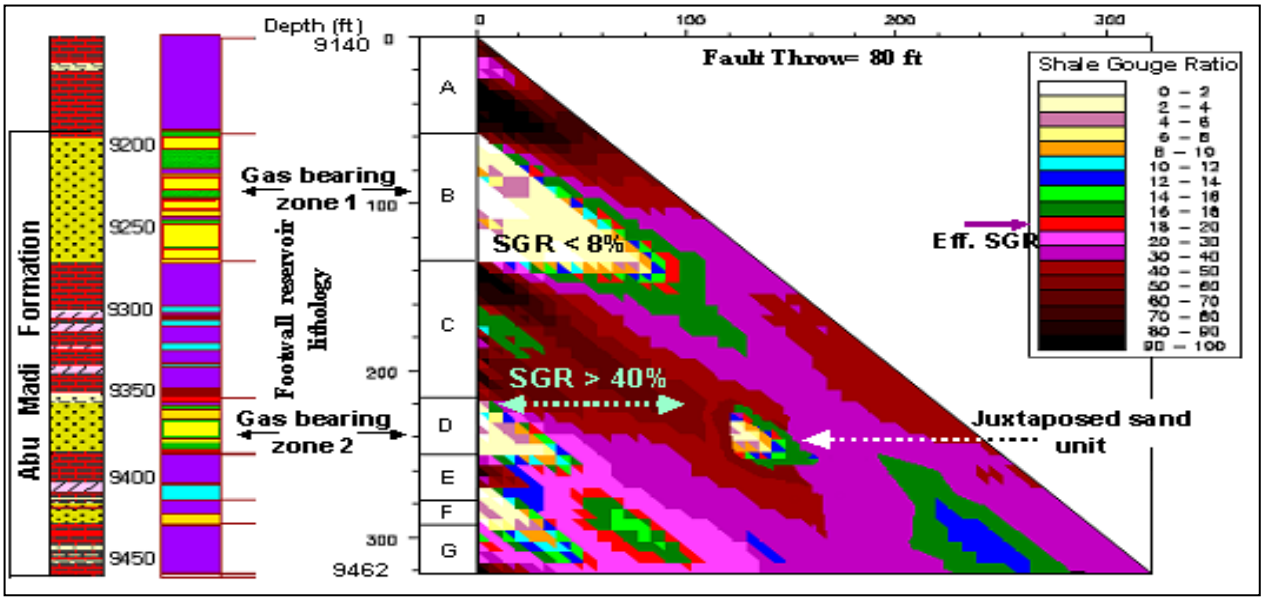

Fig. (12): Shale gouge ratio diagram of W. Abu Qir area (FW).

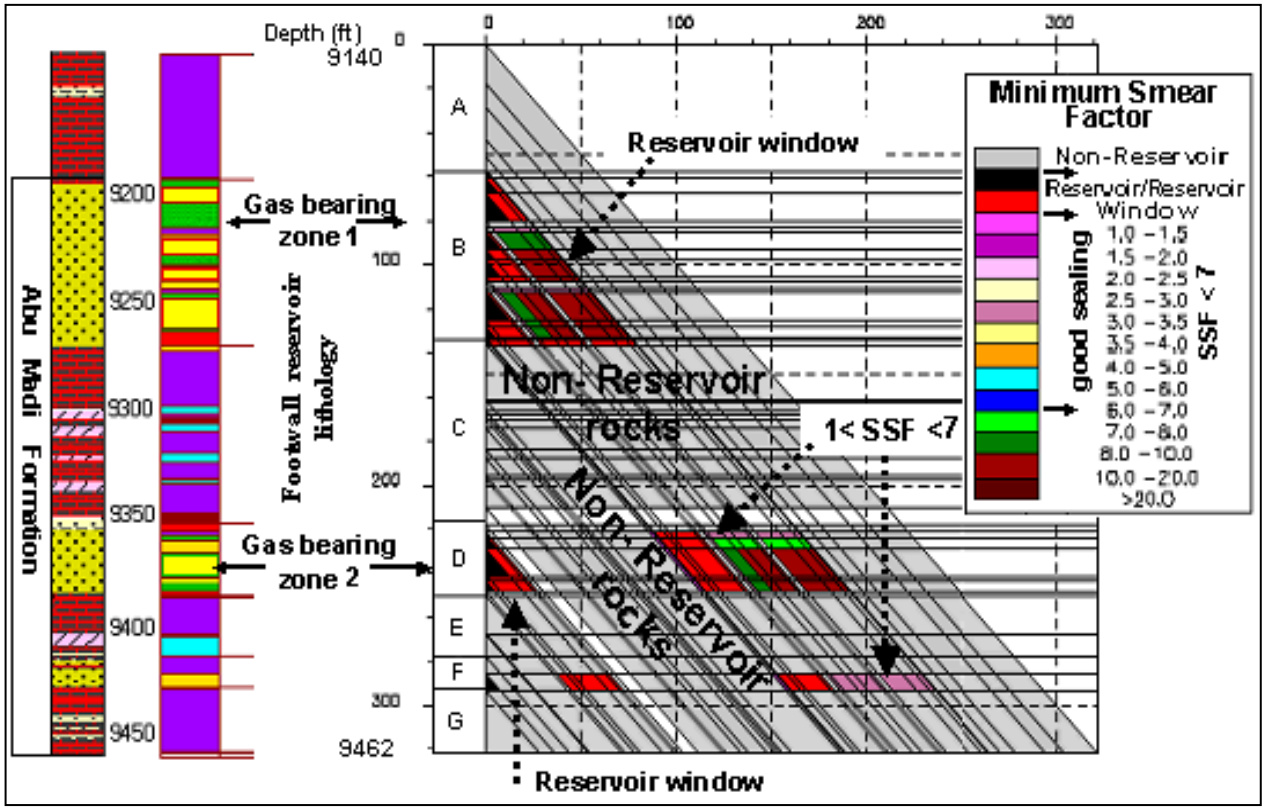

Fig. (13): Minimum smear factor diagram of W. Abu Qir area (FW).

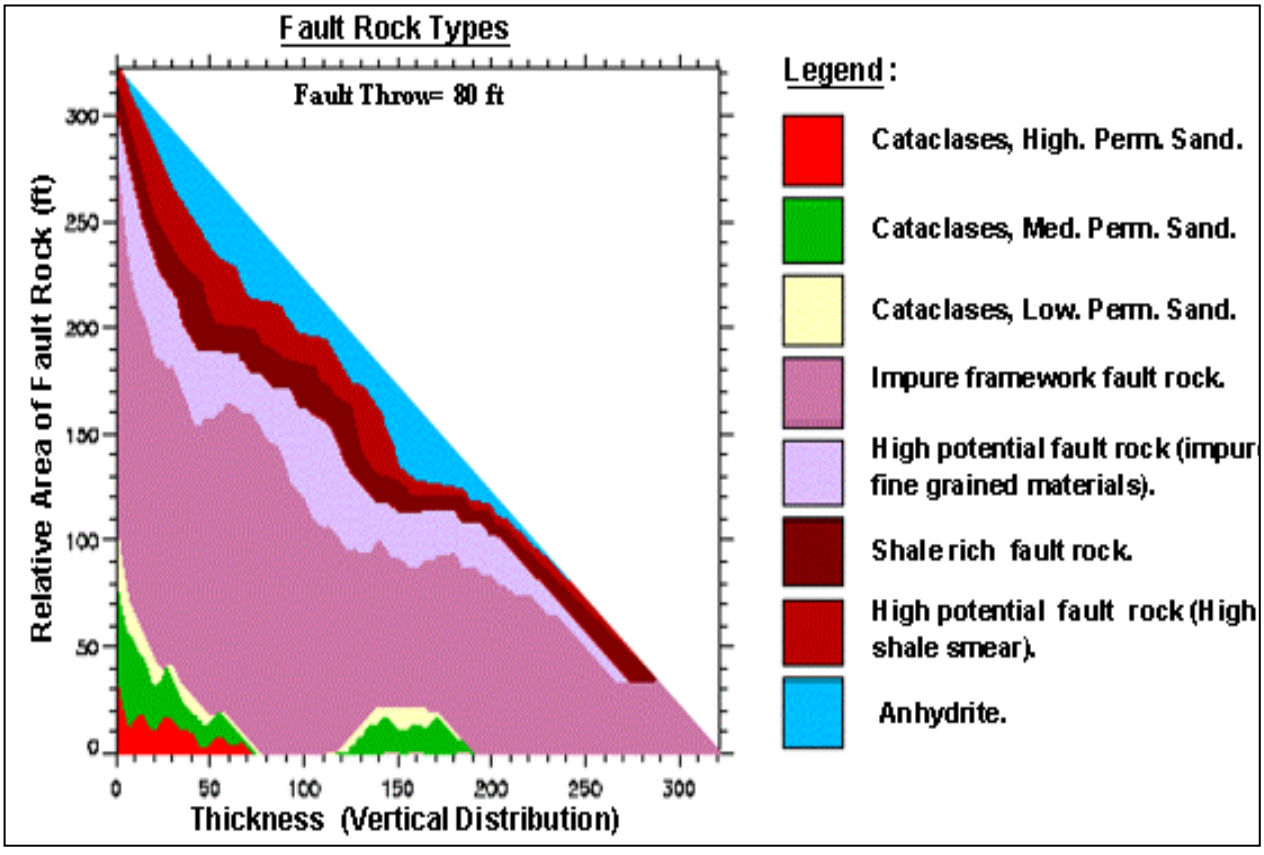

Fig. (14): Relative areas of fault rock diagram of W. Abu Qir area (FW).

1. Petrophysical Analysis

The petrophysical analysis of the Abu Roash G Member reservoir indicates the presence of two clean oil-bearing zones (mainly sandstone in composition) in the upper and middle parts of the member.

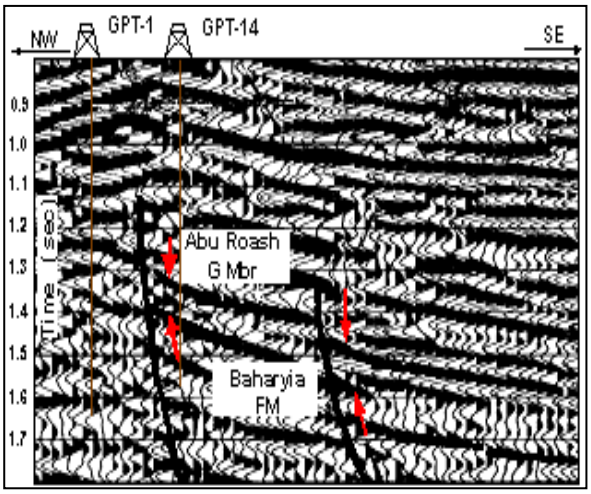

Fig. (15): Seismic section cutting through the study wells in Abu Sennan area.

These two zones are characterized by their low shale volume, good effective porosity and permeability (Fig. 16). The most important petrophysical parameters of the two studied wells are averaged in Table (2).

Table (2): The average petrophysical parameters of the hydrocarbon bearing zones in GPT-1 and GPT-14 wells.

Well	Zone	Depth (m)	Petrophysical Analysis			
			V_{sh}	ϕ_e	S_w	S_H
GPT-1	Z1	1778-1799	0.02	0.24	0.46	0.54
	Z2	1876-1895	0.01	0.21	0.55	0.45
GPT-14	Z1	1832-1855	0.01	0.20	0.56	0.44
	Z2	1898-1910	0.05	0.19	0.54	0.46

2. Sealing Analysis

The rock typing of Abu Roash G Member in the Abu Sennan area (GPT field) shows that this reservoir consists mainly of sandstone, shales and minor limestone interbeds. Six units were recognized as shown in the left side of Fig. (17). Petrophysically, units B, D and F are the best zones in the member as they exhibit low shale volume, good porosity and permeability.

Good hydrocarbon saturations are detected only in units B and F. The juxtaposition diagram (Fig. 17) shows that high to low permeable sand units not past other lithology in the HW and FW are detected in front of the units B and F. Another two medium to low permeable sand units at depths 1840m and 1880m (units D and F) in the HW are juxtaposed past other lithology of B and D units in the FW.

The sealing diagram (Fig. 18) illustrates that the framework of the fault rock is mainly phylosilicates which are impure shale in the HW or FW. Phylosilicate rich fault rock with high clay smear potential is found in juxtaposition with unit E in HW and perform good sealing diagonally along the fault plane for the lower oil-bearing zone (unit F).

Figure (19 A&B) shows the 3-D permeability and sealing capacity diagram regarding the footwall lithology. The 3-D permeability diagram attains values up to 2.5 mD ranging from low to medium permeability bars in front of the oil bearing zone-1 (unit B) and high permeability bars in front of oil-bearing zone-2 (unit F). Some medium to low permeable sand units are juxtaposed and facing other lithology especially in the lower zone. Low comparative permeability (rhomb shaped) of the limestone lithology is shown also in the base of the diagram. The 3-D sealing diagram on the other hand, shows the very high sealing capacity of the high smear shale which filling diagonally the fault wall lithology and completely seals the lower oil zone from the other lithology in the HW.

The shale gouge ratio diagram (Fig. 20) shows that much higher SGR (exceeds 50%) is given for this high smear shale which has high sealing capacity. Other fault wall lithology attains SGR values ranging between 20% and 40%. Moreover, the minimum smear factor diagram (SSF) gives reservoir/reservoir window in front of the two oil-bearing zones (Fig. 21). Low smear factor values ranging from 1 to less than 7 are recorded for the juxtaposed sand units. The other fault wall components are composed of non-reservoir lithology which have low SSF and high clay smear potential. The relative fault area diagram (Fig. 22) shows that impure framework materials are the most dominant lithology, then comes (with little percent) shale rich fault rock, high potential fault rock and finally limestone.

The Abu Madi Formation was studied in a number of wells selected to be on either sides of dissecting normal faults in some cases and neighboring pre-existing paleo-highs in anothers. These wells are El Qar'a-2 and Abu Madi-9, Abu Madi-5 and Abu Madi-12. Moreover, Khilala-1X well which is drilled on a structural culmination within a big channel system, was studied also as good example of sealing due to the combined effect of the stratigraphic/structural control.

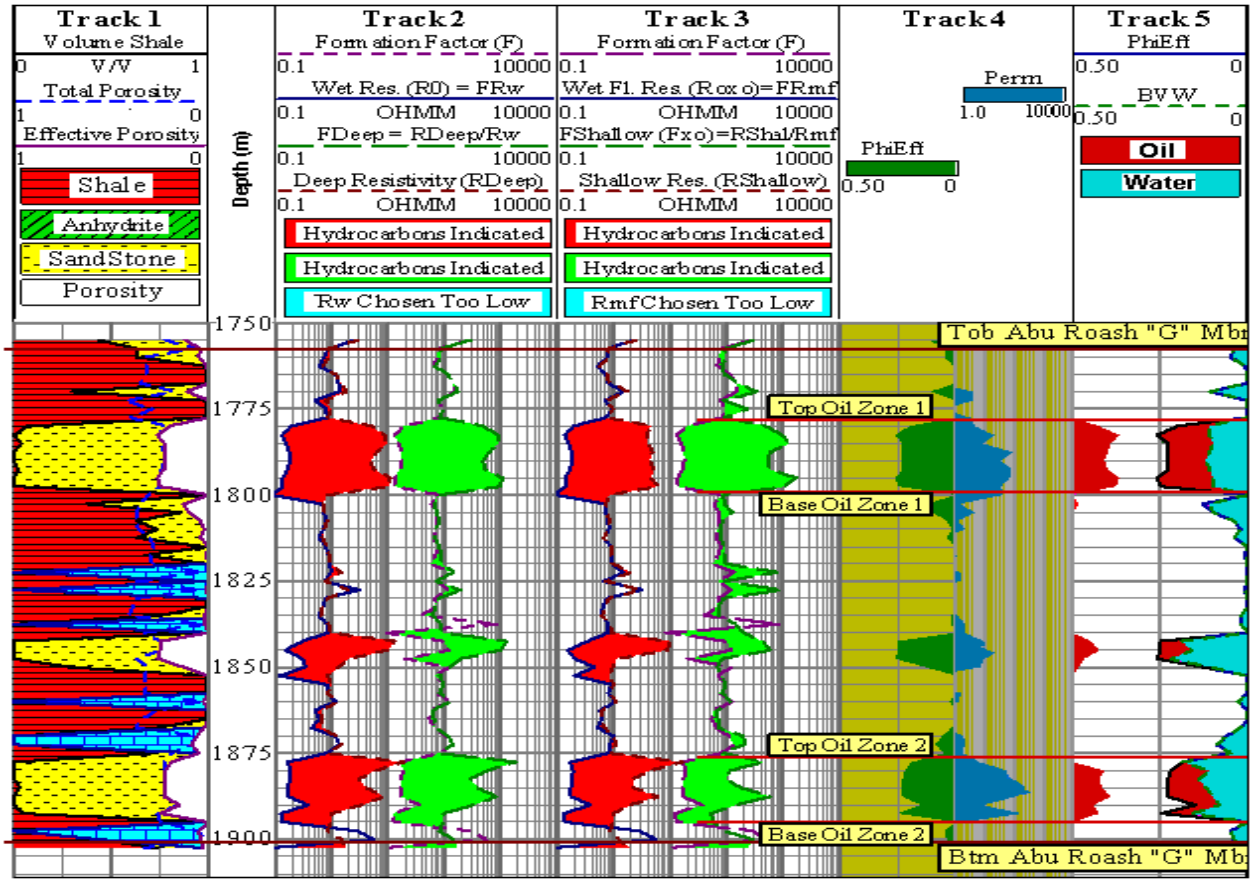

Fig. (16): Petrophysical analysis of GPT-1 well.

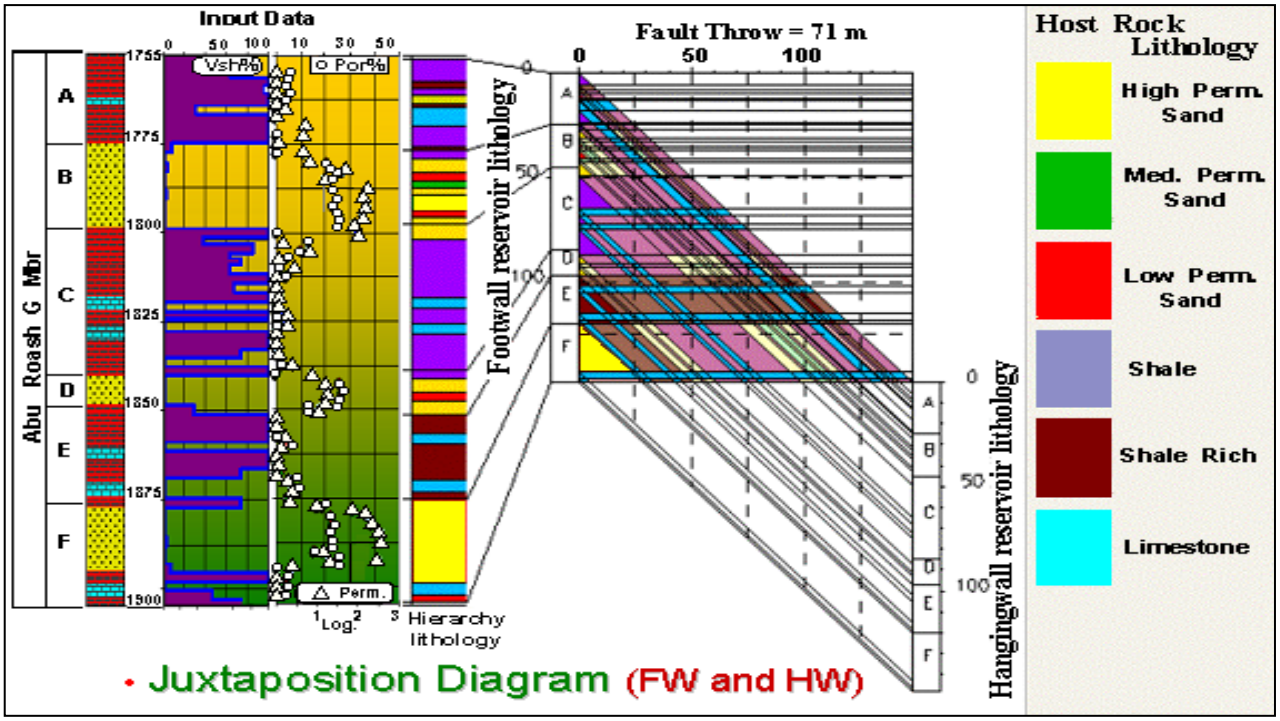

Fig. (17): Juxtaposition diagram of Abu Sennan area.

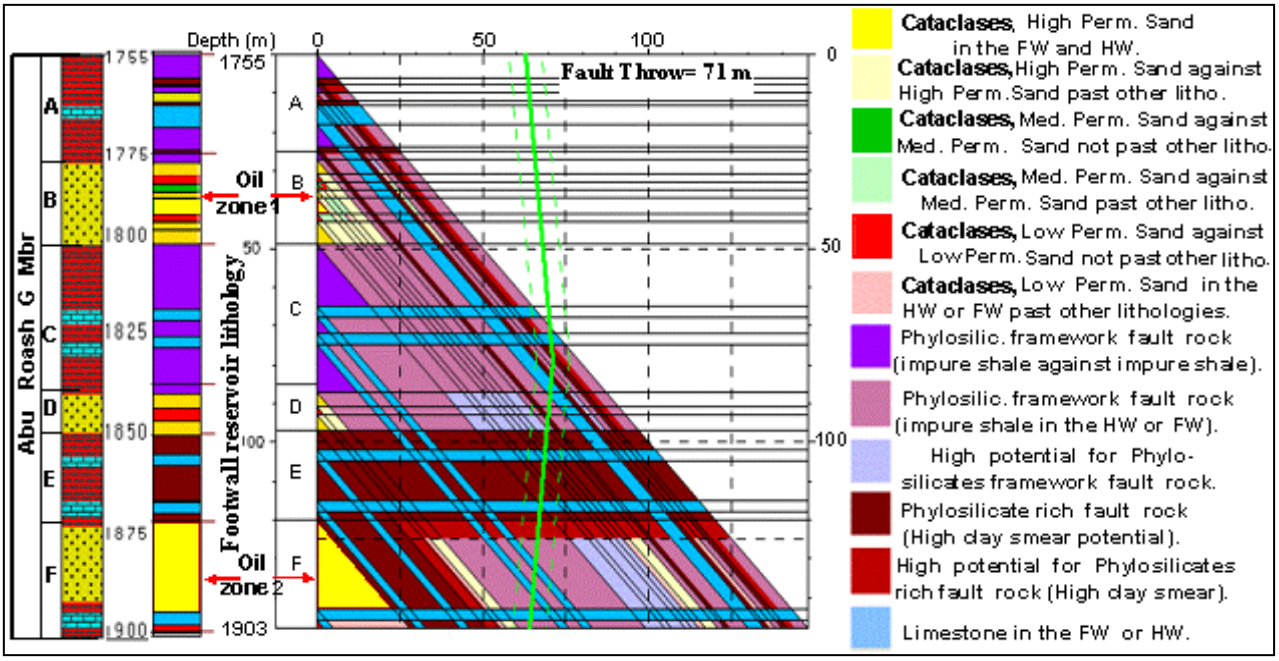

Fig. (18): Sealing capacity diagram of Abu Sennan area (FW).

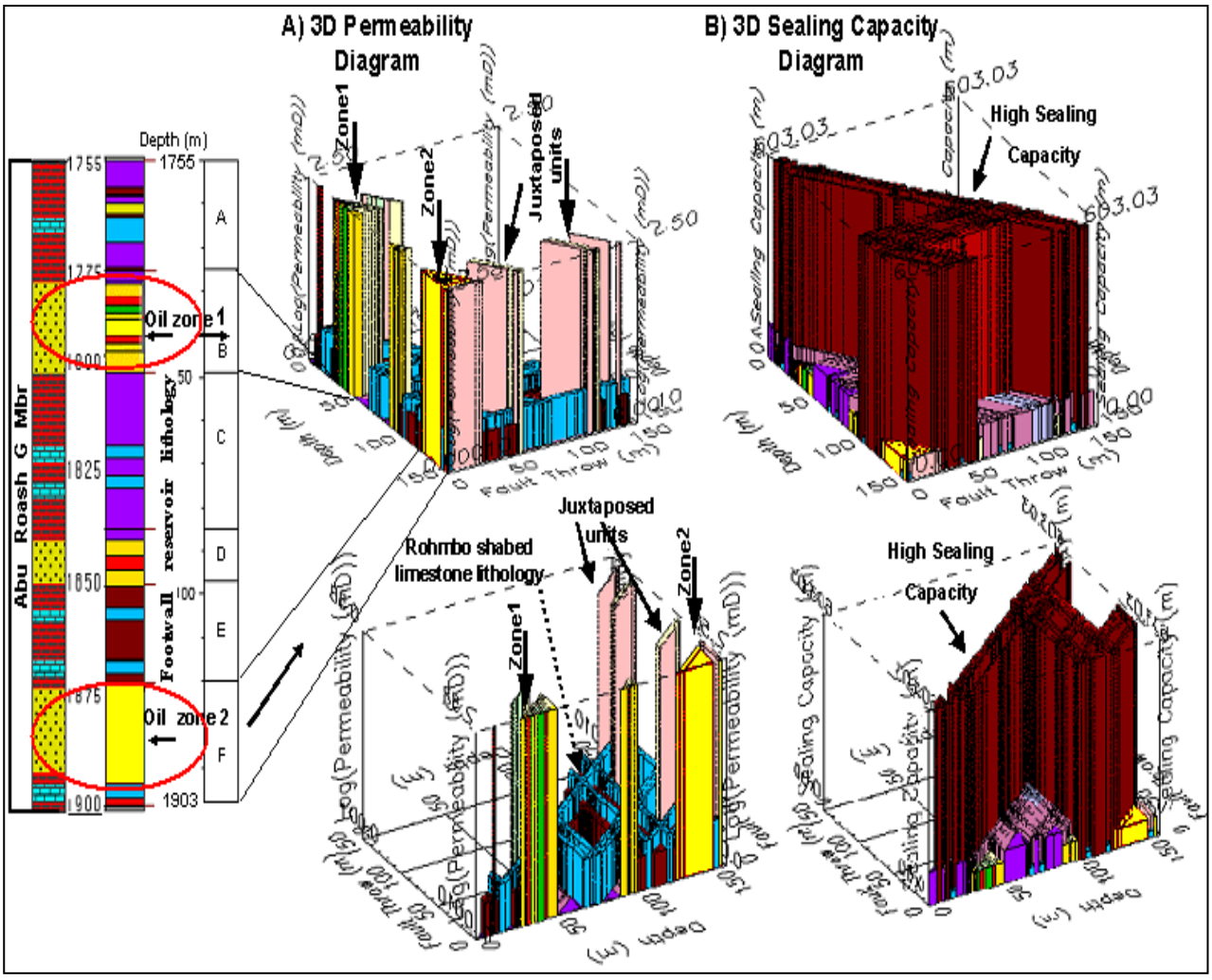

Fig. (19): 3-D permeability and sealing capacity diagrams of Abu Sennan area (FW).

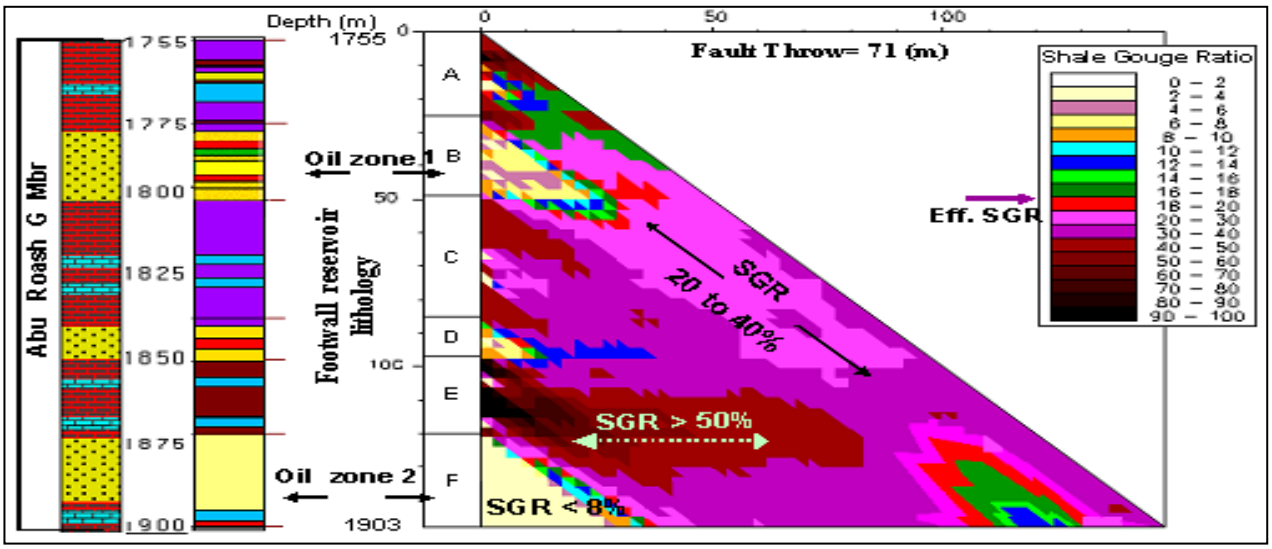

Fig. (20): Shale gouge ratio diagram of Abu Sennan area (FW).

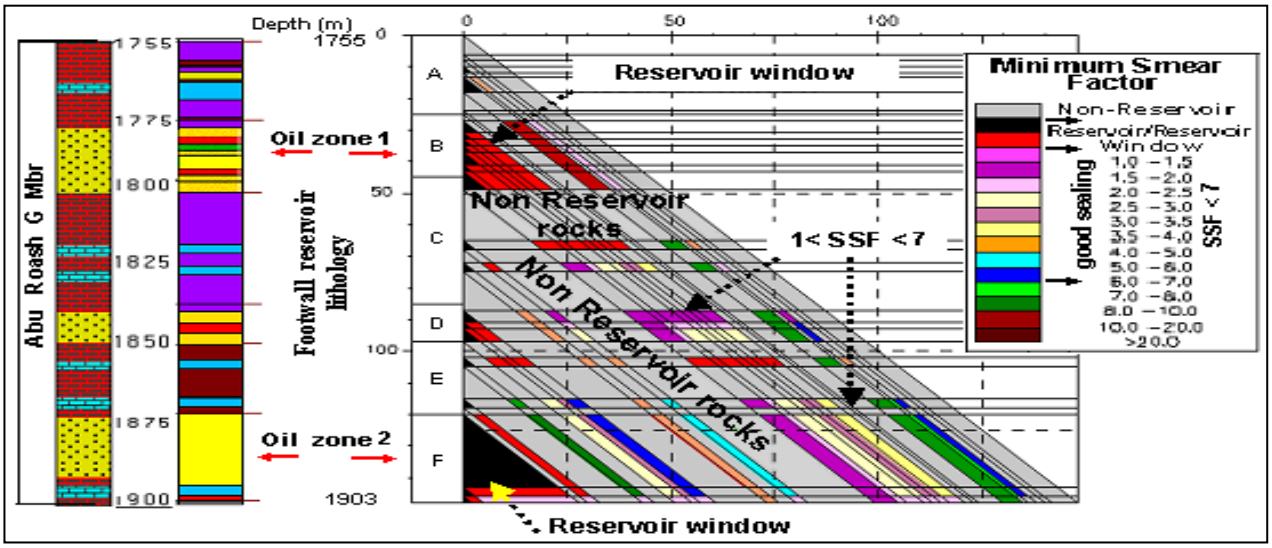

Fig. (21): Minimum smear factor diagram of Abu Sennan area (FW).

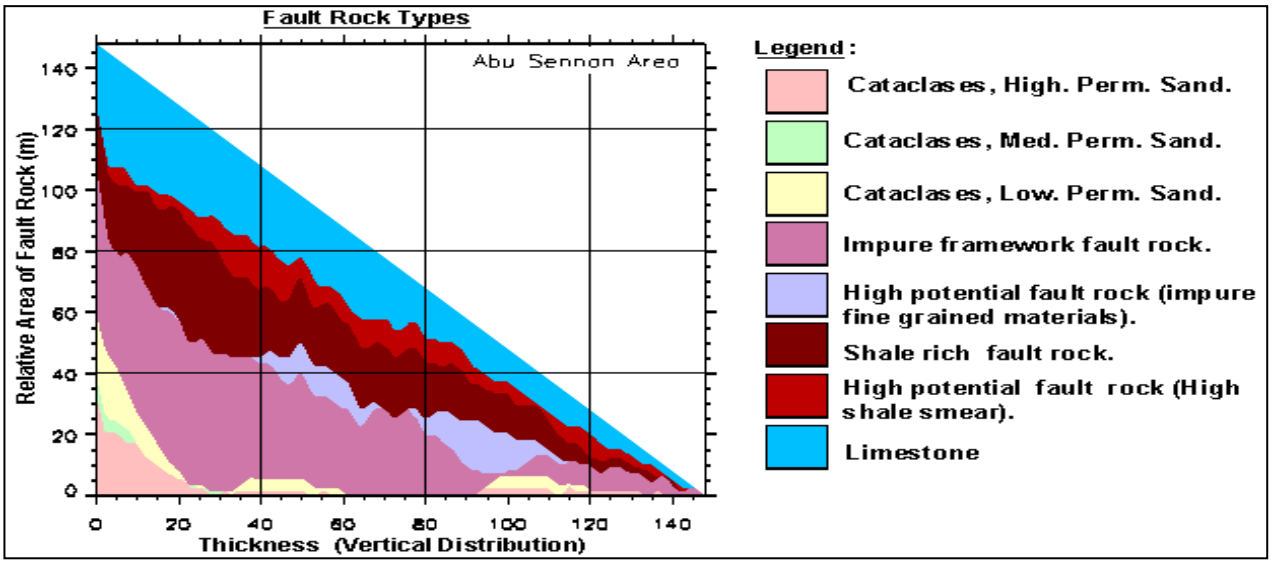

Fig. (22): Relative areas of fault rock diagram of Abu Sennan area (FW).

CASE 3: ABU MADI-El QAR'A GAS FIELD

Abu Madi is a giant field discovered in 1967 by IEOC and put in production in 1975. El Qar'a field was drilled in 1985 to the north of Abu Madi field. It was found that Abu Madi and El Qar'a were the same field (EGPC, 1994). The hydrocarbons are mainly gas and condensate entrapped in the Messinian Abu Madi Formation and sealed by the Pliocene Kafr El Sheikh clays. The production comes from two main sandstone reservoirs (level II and level III) and the trap seems to be structural and stratigraphic combination.

Sealing in this area seems to be controlled mainly by the stratigraphic condition of the reservoir of interest beside the structural configuration of the underlying sediments. In certain areas of Abu Madi-El Qar'a field, the presence of paleo-highs created by the Pre-Messinian active structures and the termination of the underlying Qawasim Formation towards these paleo-highs, represent good example.

1. Petrophysical Analysis

Only one gas-bearing zone (level III sand) is detected in the Abu Madi Formation in each of the studied wells. The petrophysical analysis reveals that thin gas-bearing reservoir of bad quality 10 m (33ft) is detected at Abu Madi-9 well at depth 3325 m (10909ft), while more thick sand zones of good hydrocarbon saturation are found at depths 3290 m (10794 ft) and 3244 m (10643ft) in El Qar'a-2 and Abu Madi-5 wells, respectively. Fig. (23) shows the petrophysical analysis of the gas-bearing sand in El Qar'a-2 well, as an example.

On the other hand, Abu Madi Formation in Khilala-1X well, consists of many sand and shale beds of fluviatile environment. Gases are detected only in the sands of level II. Table (3) summarizes the average deduced petrophysical parameters for the study wells in Abu Madi-El Qar'a area.

Table (3): A list of the average shale volume, effective porosity, water and gas saturations detected in the study wells in Abu Madi-El Qar'a area.

Well	Depth (m)	Petrophysical Analysis			
		V_{sh}	ϕe	S_W	S_H
Abu Madi-9	3325-3335	0.08	0.15	0.62	0.38
El Qar'a-2	3295-3362	0.11	0.13	0.47	0.53
Abu Madi -5	3244-3312	0.09	0.19	0.38	0.62
Khilala-1	3113-3133	0.10	0.16	0.56	0.44

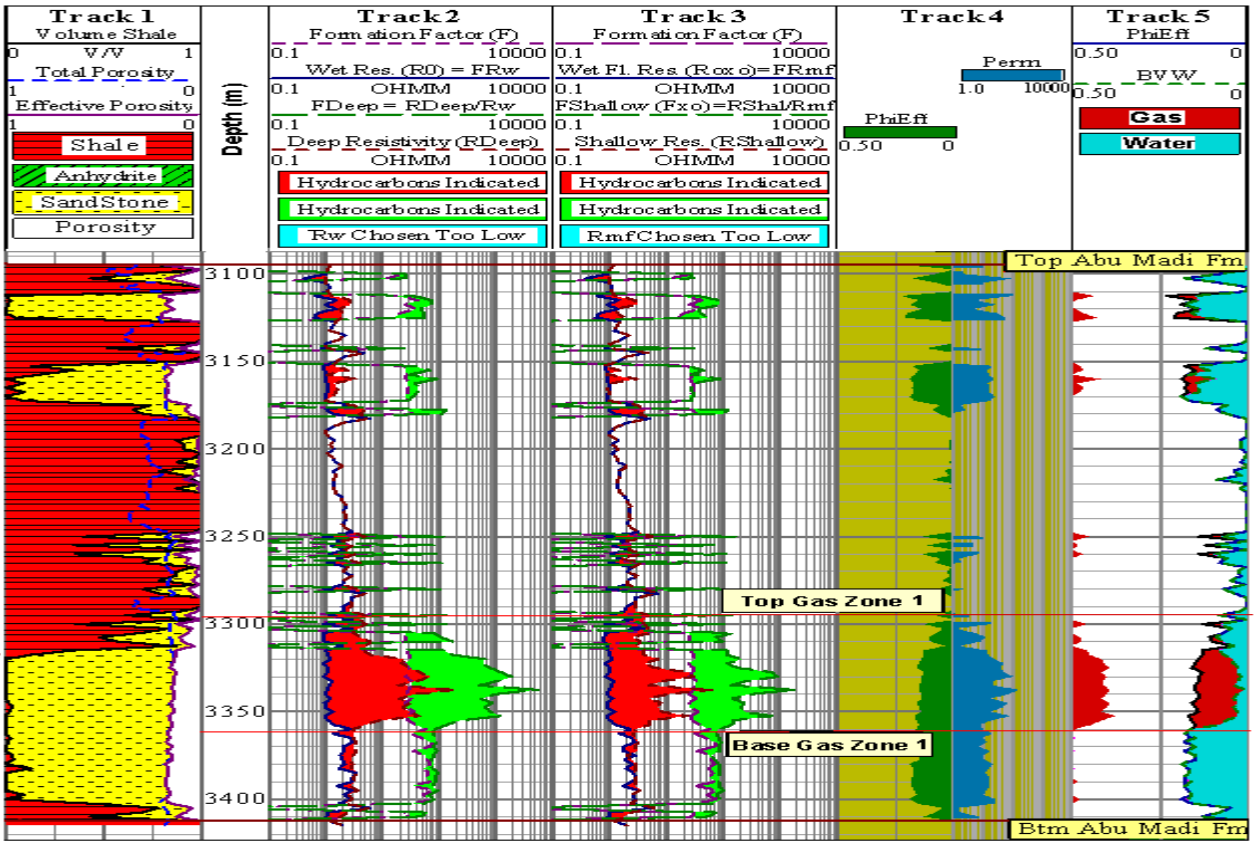

Fig. (23): Petrophysical analysis of El Qar'a-2 well.

2. Sealing Along Paleo-Highs

Paleo-highs play an important role in creating and supporting sealing potential. Two examples were studied where paleo-highs control the deposition and sealing of the hydrocarbon bearing zones. The first is found between the El Qar'a-2 and Abu Madi-9 wells (Fig. 24) where Abu Madi Formation (level III) was deposited with different thicknesses and at different depths, in both sides of locally uplifted Qawasim Formation. Two gas zones of different thicknesses and with different gas-water contacts were detected on either side of the Qawasim uplift. A stratigraphic sealing cap is provided by the overlying shale beds which enable their entrapment, but what is actually keeps these gases entrapped and prevent their escaping along either side of the uplift planes, is the sealing characteristics of the bounding faults.

For his purpose, sealing capacities (Fig. 25 A&B) were examined along the reservoir parts which just facing and affected by the fault plane.

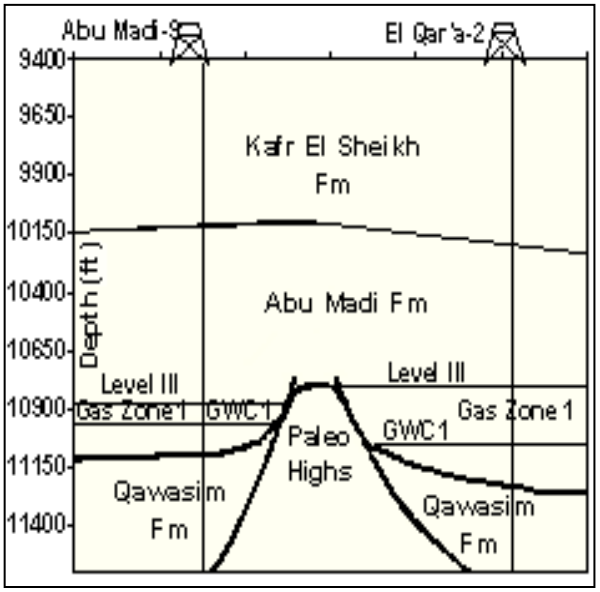

Fig. (24): Schematic geologic cross section between El Qar'a-2 and Abu Madi-9 wells.

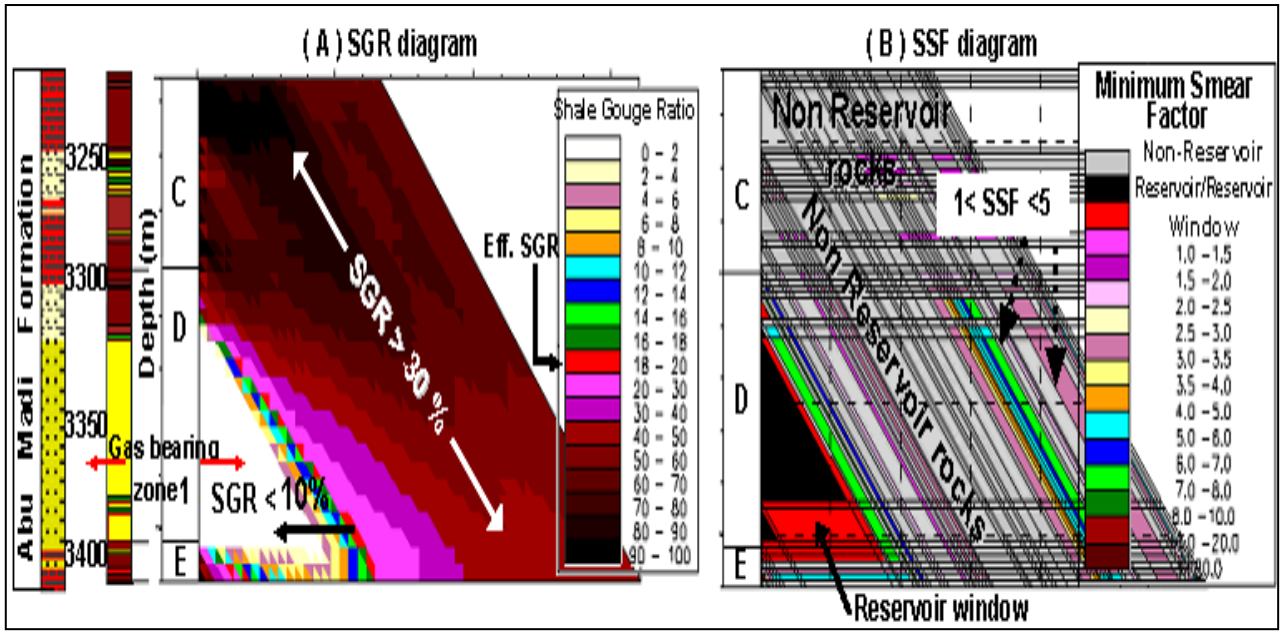

Fig. (25): Sealing parameters along the fault bounding El Qar'a-2 well; **(A) SGR diagram and (B) SSF diagram.**

Figure (25) exhibits the estimated shale gouge ratio (SGR) and the minimum smear factor (SSF) diagrams regarding the reservoir part of the Abu Madi Formation, El Qar'a-2 well. Good sealing (SGR > 30%) was recorded in the fault wall lithology which is bounding the gas-bearing zone. The smear factor diagram supports the sealing capacity of this zone (SSF < 5) and gives very low shale smear factor and non-reservoir characteristics for this faulted zone.

Another example for the sealing capacity of the bounding faults along the paleo-highs is shown in schematic geological cross section Fig. (26) where the Qawasim Formation is uplifted between Abu Madi-5 well and Abu Madi-12 well. The gas-bearing sand of level III was detected in Abu Madi-5 well only. The gas-water contact at this well is detected at depth 3364m. The combined sealing effect appears clearly in this example, where gas sand of level III is deposited in only one side and stratigraphically sealed by the overlying shale beds (stratigraphic control).

The bounding faults which structurally uplift the underlying Qawasim Formation, provide also good sealing efficiencies (SGR >20% and SSF <5) due to the closed nature of their planes.

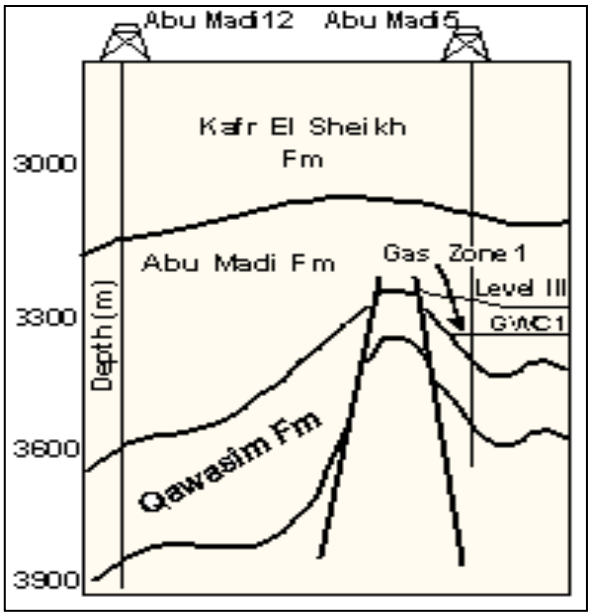

Fig. (26): Schematic geologic cross section between Abu Madi-5 and Abu Madi-12 wells.

3. Sealing Along Paleo-Lows (Channel Fills)

The interpreted seismic section passing through Khilala-1X well (Fig. 27 A) shows that the Abu Madi Formation is deposited within a big channel system in a graben shaped area bounded by faults in both sides. The rock sealing parameters (SGR and SSF) were measured along these bounding faults to check if they could or couldn't enable hydrocarbon migration.

It is found that the rock sealing capacities along these faults are so high and that these faults are closed systems (Fig. 27 B). High shale gouge ratio (SGR > 38) and low shale smear factor (SSF < 5) values were detected along the planes of these faults.

CALIBRATION OF SEAL PARAMETERS WITH PRESSURE DATA

Making use of the pressure data on either side of a fault, a more quantitative analysis can be performed. Where reservoirs are juxtaposed at the fault plane, the difference between the two pressure profiles is the pressure difference (Δp) across the fault which could or could not enable sealing. So, pressure differences across faults (Δp) of known SGR, derived from RFT measurements, can be used to calibrate the results of shale gouge algorithm. Sperrevik et al. (2002) found that fault gouge with a high clay proportion is the most effective inhibiter of hydrocarbon flow. Yielding (2002) suggested that an SGR>15% indicates that a shaly or clay-rich gouge predominates in the fault, where as SGR<15% indicated a clay-poor fault gouge.

Fig. (28) shows the cross fault pressure difference profile of W. A. Qir-1X and W. A. Qir-4X wells in West Abu Qir gas field, as correlated with the geological cross section and SGR-Depth plot. The two gas-bearing zones are detected on either side of the fault plane at different depths. At the upper gas zone, the hangingwall and footwall reservoirs overlap partly along the fault plane, while in the lower zone the reservoirs are juxtaposed against other lithology.

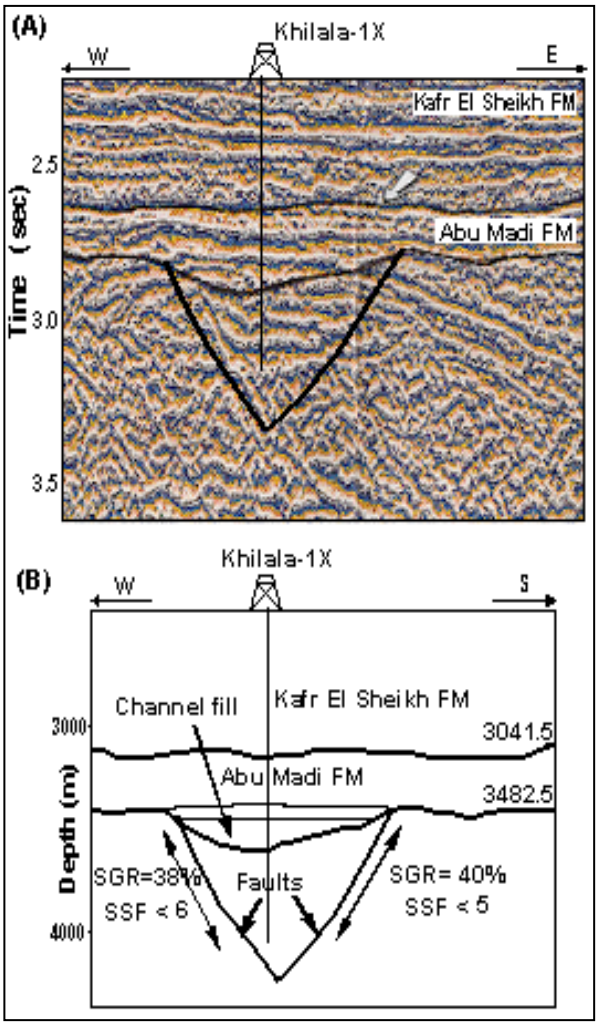

Fig. (27): A) Seismic section passing through Khilala-1X well and B) Schematic geologic cross section.

The pressure difference along the fault plane for the two gas-bearing zones reaches 70 psi.

On the other hand, the pressure difference profile (Fig. 29) of the two studied wells in Abu Sennan area exhibits a wide range of pressure difference along the fault plane due to the high fault throw, which reaches to about 80 m. The pressure gradient is found to be 0.303 which is the gradient of oil with specific gravity of 0.7 API. Reservoir to reservoir overlap is not detected on either side of the fault plane.

Good sealing capacities are characterizing this area as indicated by the high cross fault pressure difference (Δp) which the comparable oil zones attain (up to 90 psi) and the high recorded SGR values along the fault plane especially in the middle section of GPT-1 well (upthrown side). This section is composed mainly

of shale and thin limestone interbeds and exhibits much higher recorded shale gouge ratio (SGR > 40%), high sealing capacity and low permeability values (as appears in the 3-D sealing and permeability diagrams). A double effect is exhibited by this zone which acts, from one hand, as a good lithological seal separating the two oil-bearing zones in the upthrown side, and as a good juxtaposing inhibiter just facing the oil-bearing zone-1of GPT-14 well in the downthrown side of the fault, on the other hand.

The relationship between the differential pressure (Δp) and the calculated SGR and SSF values regarding the different studied areas is illustrated in Fig. (30 A and B). Comparison of the calculated attribute for the different oil and gas-bearing zones shows strong similarities in the inferred relationship between the attribute and sealing capacity. For all zones, the seal threshold for the trapped oil and gas is in the order of more than 17% SGR and less than 7 SSF values.

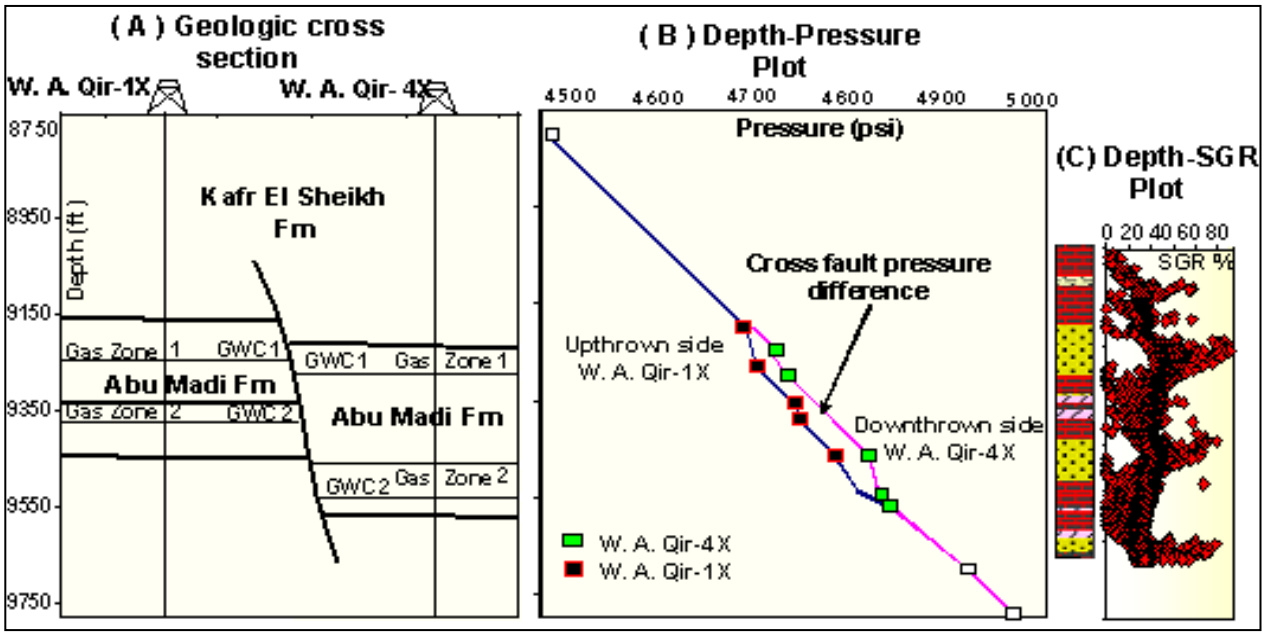

Fig. (28): Cross fault pressure difference profile as correlated with the geological cross section and SGR-Depth plot of West Abu Qir gas field.

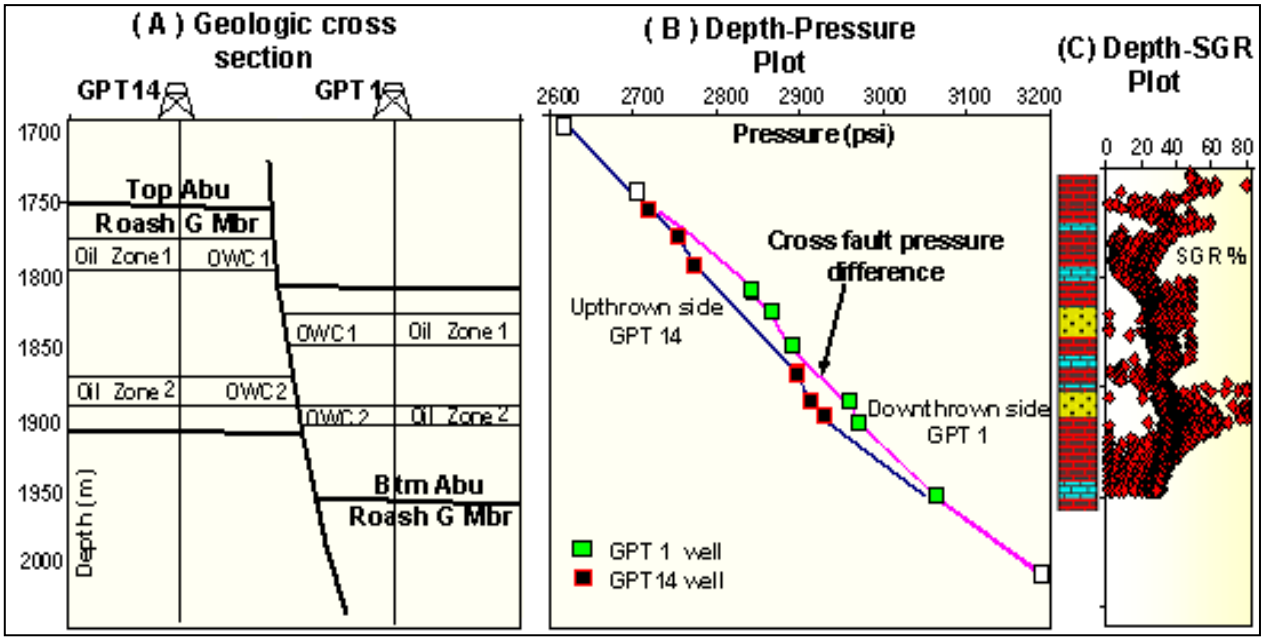

Fig. (29): Cross fault pressure difference profile as correlated with the geological cross section and SGR-Depth plot of Abu Sennan area.

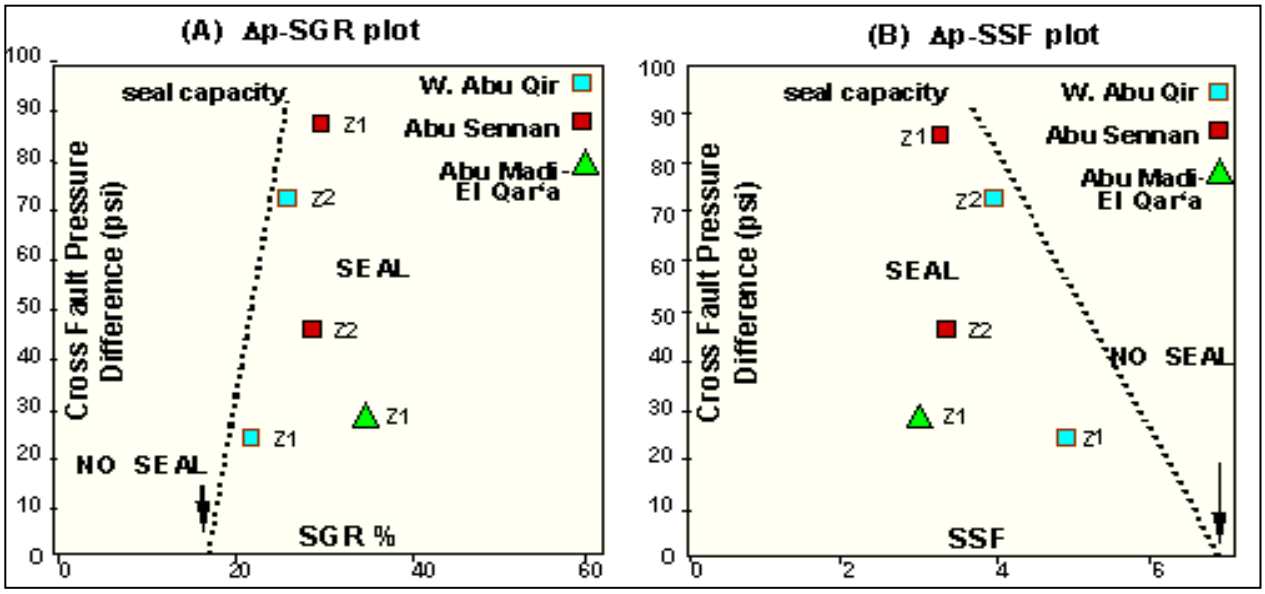

Fig. (30): The relationship between the differential pressure (Δp), the calculated SGR and SSF values regarding the different studied areas.

Some differences in the calibrations are observed between the three studied areas depending on many factors. For example, while the oil bearing-zone-1 of Abu Roash G Member (Abu Sennan area) represents the highest cross fault pressure difference, it shows SGR value (about 30%) slightly more or less than the other values recorded for the other zones which may have much lower Δp (e.g. SGR=36 and Δp=28 psi for the gas bearing zone-1 of Abu Madi -El Qar'a area).

SUMMARY AND CONCLUSIONS

Fault seal analysis was carried out over some mixed clastic reservoir rocks in three different cases in the Western Desert and Nile Delta. In some cases sealing is controlled mainly by the faults (structure control) as in West Abu Qir and Abu Sennan fields, while in other cases sealing is controlled by the combined effect of the stratigraphic and the structural condition of the reservoir of interest as in Abu Madi-El Qar'a area, (paleo-highs or paleo-lows).

Rock typing was performed using different methods especially the hierarchical method. Juxtaposition diagrams were constructed and some important fault seal related parameters were estimated (SGR, CSF, SSF, Δp,…etc). Also, different 3-D sealing capacity and permeability diagrams were constructed.

Complete petrophysical analysis was carried out in each area using two wells drilled on both sides of the fault (footwall and hangingwall) to detect the hydrocarbon bearing zones. Fault parameters (type of fault, dip angle, direction and magnitude of throw) were gathered from the interpreted seismic sections. The petrophysical analyses of the selected wells revealed the presence of two gas and oil-bearing zones of different pressure differences along the fault planes in W. Abu Qir and Abu Sennan areas. Meanwhile, only one gas-bearing zone was detected in the studied wells in Abu Madi-El Qar'a area.

The sealing analysis clarified that the sealing threshold attributes which could differentiate between sealing and non sealing efficiencies along the studied faults regarding the reservoir rocks in the different studied cases, can be considered in the order of more than 20% SGR and less than 7 SSF values. Some relative differences were found between the deduced sealing capacities in the oil and gas-bearing zones.

Moreover, pressure data were also incorporated and used to calibrate the concluded seal attributes along the fault planes. Cross fault pressure difference (Δp) was used as a measure for the efficiency of the sealing attributes. Good cross fault pressure differences were found in association with good and high rock sealing parameters (high SGR and low SSF).

REFERENCES

Allan, U. S. (1989): Model for hydrocarbon migration and entrapment within faulted structures. APPG Bulletin, v. 73, p. 803-811.

Bouvier, J. D., Kaars-Sijpesteijn, C. H., Kluesner, D, F., Onyejekwe, C. C. and Van der Pal, R. C., (1989): Three-dimensional seismic interpretations and fault sealing investigations, Nun River field, Nigeria. APPG Bulletin, v. 73, p. 1397-1414.

Chapman, T. J. and Maneilly, A. W. (1990): Fault displacement analysis in seismic exploration. First Break, v. 8, p. 11-22.

EGPC, (1994): Nile Delta & North Sinai fields, discoveries and hydrocarbon potentials (a comprehensive overview). The Egyptian General Petroleum Corporation, Cairo, Egypt, 387 P.

Freeman, S., Harris, S., Kinpe, R. J., and Davies, R. (2004): Rapid approaches to mapping and interpreting fault seal properties within reservoir modeling packages. Ex. Abs., 19th April, APPG annual convention, Dallas.

Fulljames, J. R., Zijerveld, J. J., Franssen, R. C. M. W., Ingram, G. M., and Richerd, P. D. (1996): Fault seal processes, in Norwegian Petroleum Society, eds., Hydrocarbon seal- Importance for exploration and production. (conference abstracts) Oslo, Norwegian Petroleum Society, p. 5.

Gauthier, B. D. M. and Lake, S. D. (1993): Probabilistic modeling of faults below the limit of seismic resolution in Pelican field, North Sea, Offshore United Kingdom. APPG Bulletin, v. 77, p. 761-777.

Harding, T. P. and Tuminas, A. C. (1989): Structural interpretations of hydrocarbon traps sealed by basement normal blocks and at stable flank of fore-deep basins and at rift basins. APPG Bulletin, v. 73, p. 812-840.

Harris, D., Yielding, G., Levine, P., Maxwell, G., Rose, P. T. and Nell, P. (2002): Using of shale gouge ratio (SGR) to model faults as transmissibility barriers in reservoirs: An example from the Strathspey field, North Sea. Petroleum Geoscience, v. 8, p. 167-176.

Hills, R. R. and Jones, R. M. (2003): An integrated, quantitative approach to assessing fault seal risk. APPG Bulletin, v. 87-3, p. 507-524.

Jev, B. I., Kaars-Sijpesteijn, C. H., Peters M. P. A. M., Watts, N. L., and Wilkie, J. T. (1993): Use of integrated 3-D seismic fault-slicing, clay smearing and RFT pressure data on fault trapping and dynamic leakage, Akaso field, Nigeria. APPG Bulletin, v. 77, p. 1389-1404.

Kinpe, R. J., (1992a): Faulting processes, seal evolution and reservoir discontinuities: An integrated analysis of the ULA field, central graben, North Sea. Abstracts of the petroleum group meeting on collaborative research programme in petroleum geosciences between UK higher education institutes and the petroleum industry, the Geological Society of London.

Kinpe, R. J., (1992b): Faulting processes and fault seal. In: Larsen, R. M, ed., Structural and tectonic modeling and its applications to petroleum geology. NPF, Stavanger, p. 325-342.

Kinpe, R. J., (1993b): Micromechanisms of deformation and fluid flow behaviour during faulting. In: The mechanical behaviour of fluids in fault zones. U.S.G.S. Open file report 94-228, p. 301-310

Kinpe, R. J., (1997): Juxtaposition/ seal diagrams to facilitate fault seal analysis of hydrocarbons. APPG Bulletin, v. 81-2, p. 187-195.

Kinpe, R. J., Freeman, S., Harris, S., and Davies, R. (2004): Structural uncertainty and scenario modeling for fault seal analysis. Ex. Abs., 20th April, APPG annual convention, Dallas.

Lindsay, N. G., Murphy, F. C., Walsh, J. J., and Watterson, J. (1993): Outcrop studies of shale smear on fault surfaces. International Associations of Sedimentologists, Special Publication 15, p. 133-123.

Sperrevik, S., Gillepsie, P. A., Fisher, Q. J., Halvorson, T. and Knipe, R. J. (2002): Empirical estimation of the fault rock properties. In: Koestler, A. G. and Hundsdale, R. (eds). Hydrocarbon seal quantification. NPF special publication, 11, Elsevier, Amsterdam.

Watts, N. (1987): Theoretical aspects of cap-rock and fault seals for single-and two-phase hydrocarbon columns. Marine and Petroleum Geology, v. 4, p. 274-307.

Weber, K. J., Mandl, G., Pliaar, W. F., Lehner, F., and Precious, R. G. (1978): The role of faults in hydrocarbon migration and trapping in Nigerian growth fault structures. Offshore technology Conference 10, paper OTC 3356, p. 2643-2653.

Yielding, G. (2002): Shale gouge ratio-Calibration by geohistory. Norwegian Petroleum Society, NPF special publication 11, p.1-15.

Yielding, G., Badley, M. E. and Roberts, A. M. (1992): The structural evolution of the Brent province. In: Morton, A. C., Haszeldine, R. S., Giles, M. R. and Brown, S., (eds). Geology of The Brent Group. Geological Society, London, Special Publications, 61, p. 27-43.

Yielding, G., Freeman, B., and Needham, T. (1997): Quantitative fault seal prediction. APPG Bulletin, v. 81-6, p. 897-971.

Yielding, G., Overland, J. A. and Byberg, G. (1999a): Characterization of fault zones in the Gullfaks field for reservoir modeling. In: Fleet, A. J. and Boldy, S. A. R. (eds), Petroleum Geology of Northwest Europe. Proceedings of the 5th Conference. Geological Society, London, p. 1177-1185.

Yielding, G., Overland, J. A. and Byberg, G. (1999b): Characterization of fault zones for reservoir modeling: An example from the Gullfaks field, Northern North Sea. APPG Bulletin, v. 83-6, p. 925-951.